LAMS-2444

C.3

LOS ALAMOS SCIENTIFIC LABORATORY

OF THE UNIVERSITY OF CALIFORNIA o LOS ALAMOS NEW MEXICO

QUARTERLY STATUS REPORT OF THE LASL
CONTROLLED THERMONUCLEAR RESEARCH PROGRAM
FOR PERIOD ENDING MAY 20, 1960

Printed in USA. Price $ 1.50. Available from the

Office of Technical Services
U. S. Department of Commerce
Washington 25, D. C.

LAMS-2444
UC-20, CONTROLLED THERMONUCLEAR PROCESSES
(TID-4500, 15th Ed.)

LOS ALAMOS SCIENTIFIC LABORATORY
OF THE UNIVERSITY OF CALIFORNIA LOS ALAMOS NEW MEXICO

REPORT COMPILED: July 1960
REPORT DISTRIBUTED: July 29, 1960

QUARTERLY STATUS REPORT OF THE LASL CONTROLLED THERMONUCLEAR RESEARCH PROGRAM FOR PERIOD ENDING MAY 20, 1960

Compiled and edited
by
Samuel Glasstone

From reports written by members of P Division

Contract W-7405-ENG. 36 with the U. S. Atomic Energy Commission

INTRODUCTION

The major topics of study are: (1) confinement of plasma in picket fence systems (cusped geometries); (2) trapping of plasma into magnetic confining systems by the entropy trapping method; (3) acceleration of plasma in various types of gun for use with the above, and studies of these guns; (4) axial compression in mirror geometry (Scylla and Orthogonal Pinch); (5) toroidal stabilized pinch (Perhapsatron S-5), loss process studies; (6) plasma rotation in crossed electric and magnetic fields in magnetic mirror geometry (Ixion); (7) plasma oscillations and observation of the modulation of a scattered microwave beam by plasma oscillations; (8) calculations of ionization and excitation cross sections; and (9) capacitor energy storage (Zeus) and component development.

During the past six months there has been a change in emphasis in the experimental program. Following the Geneva Conference, the stabilized pinch was the major experimental approach, both in number of machines (three) and in manpower. The prospects of strong cyclotron radiation losses for plasmas containing magnetic fields suggests that it will be difficult to design a thermonuclear reactor using the D-T reaction, and practically impossible to design a D-D reactor. One way to avoid this source of energy loss is to have no magnetic field in the plasma, so that the radiation is only a surface phenomenon instead

of a bulk one. Of all the currently known magnetic confining geometries, only one theoretically has enough stability to hold a pure plasma (i.e., $\beta = 8\pi\, nkT/B^2 = 1$), namely, the picket fence cusped geometry. Theory indicates that the cusps are very leaky but there may be modifications and additions by which the losses can be avoided or minimized. Consequently, the effort on the stabilized pinch ($\beta < 1$) has tapered off to one machine, and more emphasis is now being placed on picket fence geometries (two in operation).

The Entropy Trapping principle, which predicts that a plasma jet may hydromagnetically pierce a magnetic field and be trapped in a magnetic confinement system, provided the incentive to start actual construction of the cusp experiments. Such a study necessarily involves a program on gun research, to produce a plasma jet of high density and velocity. Fortunately a promising design was available in the hydromagnetic gun developed in the Laboratory.

A brief summary of the status of the experimental program is given here and further details appear in later sections of this report.

A. Entropy Trapping Experiment

The experimental results to date are encouraging. With a low-velocity plasma jet (deuteron energy ~ 200 ev, density ~ $10^{13}/cm^3$) and small magnetic fields (~ 300 gauss) the entrance cusp opens ($\beta = 1$) during the passage of the plasma and closes in 2 μsec. There apparently is no critical field such as is predicted by the simple theory, because of a focusing of the incoming jet, which raises the jet density, thereby changing the critical magnetic field from a cut-off to a more gradual throttling effect. Again at low magnetic fields and low plasma velocities the plasma is trapped in the central region with $\beta \approx 1$ in a volume of radius ~ 5 cm with a lifetime of ~ 50 μsec. However, there are two major difficulties that have been found: (a) as the velocity of the plasma jet is increased (density decreased because of gun characteristics, maintaining total energy roughly

constant), the β in the entrance cusp and midplane are strongly reduced, and (b) the plasma jet is found to consist of 50 to 90% neutral particles which pass through the picket fence magnetic field.

B. Hydromagnetic Gun

Diagnostic studies of the operation of the hydromagnetic gun have given current distributions along the gun barrel as a function of time, the axial velocity of the current sheath, evidence of the formation of an instability at low pressures, and the magnetic field distribution as the plasma jet enters a magnetic cusp.

The gun has been greatly improved in performance mainly by using a very low-inductance energy source and trimming the gun length qualitatively to give the best performance. The mean velocity of the plasma jet has been increased to $\sim 10^8$ cm/sec with a particle density of $\sim 10^{12}/cm^3$. The low density is due in part to the $\sim$ 2 meters spatial extent of the plasma jet.

Attempts to use high voltage ($\sim$ 100 kv) on a gun have so far been plagued with insulation difficulties.

C. Skew Trapping

The purpose of this experiment is to study the possibility of injecting particles into a static magnetic field system by breakdown of the adiabatic invariant of the particle motion in crossing the low-field region at the center of a picket fence. This effect can be increased by introducing a distortion or asymmetry in the two halves of the picket fence. A 30-kev deuteron beam is injected at a critical angle for entrance into the axial cusp and the two halves can be distorted by shifting the coils. The resulting motion of the beam has proved to be complicated and is not understood. No trapping has yet been detected.

D. Axial Compression Experiments - Scylla and Orthogonal Pinch

The recent work on Scylla has concentrated on preionization studies which have advanced the normal second half-cycle to first half-cycle operation. It has been shown that, in addition to heavy preionization, an anti-parallel, quasi-static magnetic field will produce neutrons on the first half cycle, while a parallel field will not. Comparison of the effects of parallel and anti-parallel fields shows that an effect of the latter in producing an active plasma occurs at an early stage of the first half-cycle, corresponding to the time of the initial sheath implosion.

The Orthogonal Pinch similar to Scylla but using lower voltage condensers (20-kv maximum) produces ~ 6 to 8 x 10^6 neutrons per discharge of duration ~ 6 to 10 μsec. Magnetic probes show the presence of a reversed magnetic field and the interdiffusion of this field with the external confining field. The effect of changing the mirror ratio has been examined and as the mirror ratio is reduced from 5:1 to 1:1 the neutron yield increases and end losses become more pronounced.

In the axial compression devices the question remains unanswered as to the magnitude of the magnetic field in the plasma at peak compression. Magnetic probes in the orthogonal pinch show diffusion of the trapped reverse field with the external confining field. In Scylla the reversed field is observed only when it is greatly increased by compression and inertial effects during the initial sheath implosion. Later, at peak compression the confining field diffuses rapidly to the central region of the probe. The consequences of the presence of the probe on the plasma temperature and conductivity are still unknown except to note that the probe does affect adversely those processes that are responsible for neutron production. In Scylla the probe also produces large quantities of contaminants with ionization states lower than are usual without the probe. To provide further information on this matter, an experiment using the Zeeman effect has been designed to measure the magnetic fields in the plasma.

E. Perhapsatron S-5

The earlier results from Perhapsatron S-4 showed that, within experimental error, ultraviolet radiation losses from impurity ions were responsible for the prohibitive energy loss from the pinch. The time of onset of the radiation was found to be controlled by the percentage of impurities in the initial gas filling. Applying this result to Perhapsatron S-5 (twice the size, same electric field gradient) the ultraviolet signal was delayed to the end of the first half-cycle ($\sim$ 35 μsec) with an increase in neutron yield ($\sim 10^8$ neutrons/discharge). In order to determine whether this improvement can be extended to higher power operation and perhaps make possible the attainment of thermonuclear temperatures, Perhapsatron S-5 is currently being adapted to operate at higher voltages, using a 1.14-megajoule section of the Zeus condenser bank with an increase in discharge current from ~ 0.3 to $\sim 0.9 \times 10^6$ amp.

F. Ixion

The voltage limiting action appears to arise from ion neutral interactions in the plasma, rather than from effects due to end insulators. The data show a rather distinct threshold velocity for the inelastic process which causes the limiting, i.e., the viscous, losses in the plasma.

G. Plasma Oscillations

This experiment is an attempt to measure the intensity, frequency spectrum, and angular distributions of microwaves scattered by an ionized gas. The scattering plasma is contained in an R.F. excited glass bottle, the primary radiation is produced by a tuneable magnetron, and the detector is a microwave radiometer. In theory the present experiment appears to be about two orders of magnitude away from detecting the radiation scattered from plasma in thermal equilibrium.

H. Ionization and Excitation Cross Sections

The ionization and excitation cross sections are being calculated for impurity atoms. With these results energy losses by radiation from impurities can be computed for deuterium plasmas in dynamic equilibrium.

I. Zeus and Component Development

Ten of the planned 42 tiers, for the first stage of the Zeus capacitor bank, have been completed and tested. Of these, nine are being hooked up to Perhapsatron S-5. Progress is being made in the development of capacitors of very low inductance, of high-voltage, high-current switches, and other components required for new research devices.

A. ENTROPY TRAPPING

The purpose of the entropy trapping experiment was to test the theory which predicts that a plasma jet may pierce a magnetic field and be trapped thereby. The plasma jet is produced by a hydromagnetic plasma gun of the type developed at LASL with modifications to give (a.) an output pulse of short time duration and (b) particles of higher energy. The magnetic confinement system has the picket fence geometry and is operated under dc conditions with a maximum magnetic field of about 15 kgauss at the mirror ends and about 12 kgauss at the line cusp. The distance between the axial cusps is 40 cm and the radial cusp has a radius of 20 cm.

Hydromagnetic Gun

Initial operation of the gun (length 60 cm, major and minor radii 4.8 cm and 2.5 cm, respectively, 20 kv and 28 μf) gave a long (about 20 μsec) duration pulse of plasma with velocities in the 10^7 cm/sec range. Before work could be done on the trapping problem it seemed advisable to improve the plasma source. Three approaches have been tried of which the first two were failures; the third approach, however, shows promise of being successful.

1) An unstable linear pinch, using the regular condenser bank, was set up with an aperture in the cathode. A search was then made for energetic deuterons which might be ejected through the apperture, the existence of such deuterons being inferred from the neutrons produced by an unstable pinch. No large flux of high-velocity deuterons

was found; rather, the aperture emitted a pulse of slow-moving plasma, with a speed at the front of 2 cm/μsec, lasting several tens of microseconds. The total energy content, measured by a thermocouple, was less than 1% of the bank energy.

2) A return to the hydromagnetic acceleration approach was then made. A gun was used in which the electrodes formed a parallel-plate transmission line 2 in. wide separated by 1/2 in.; the line termination was the plasma blob being accelerated. This gun geometry was extremely unstable, as expected, with the discharge tending to run off the sides of the electrodes. The spacing at the edge of the electrodes was reduced to provide magnetic mirrors along the side of the gun, in the hope that this might center the discharge, but there was no obvious effect upon the stability.

3) In the third approach the coaxial hydromagnetic gun was operated with a voltage supply of very low capacitance. The principal object in going to a faster system (20 kv, 1.7 μf) was to obtain a short, well-defined burst of plasma for injection into the picket fence confining field. In preliminary measurements of magnetic signals and energy output, it was found that the magnetic front showed a rapid acceleration to a velocity in the range of 4×10^7 cm/sec near the gas inlet to the gun, but little (if any) signal or energy came out of the muzzle of the gun.

From previous work it was felt that the pinching of the plasma off the end of the central electrode seemed to have a focusing action on the accelerated plasma. Hence, the central electrode of this faster coaxial gun was shortened to an effective length of about 15 cm to allow pinching of the plasma off its end before the first current zero in the discharge cycle. With this alteration, optimum energy output and velocity are found for a plenum pressure near 50 mm and a maximum voltage of 20 kv on the condenser bank. These gun conditions produce a plasma burst which exhibits a magnetic pulse with an average front

velocity of 6×10^7 cm/sec, a time duration of about 4 μsec, and a plasma kinetic energy output of 25 to 35 joules (roughly 10% efficiency) at a detector located 4 in. from the gun. A further improvement in gun performance has been achieved by increasing the frequency of the driving system.

The gun is shown schematically in Fig. 1. The main features of this design are (a) the absence of any switches and (b) the short low-inductance transmission lines feeding the discharge. These reduce the external inductance to 0.019 μh, which is 22% of that of the preceding assembly, and the first half period to ~ 0.8 μsec, which was previously ~ 1.4 μsec.

It is possible to dispense with switches in this design because the relatively low pressures in the gun prevent breakdown of the gas for a few tens of microseconds. This gives enough time to charge the condenser bank from an external Marx generator with the discharge initiated by firing a spark plug in the gas.

Observations with the gun have established the following:

1) Over 90% of the condenser energy is dissipated during the first half cycle; this is not due to any low Q characteristic of the external circuit.

2) The maximum particle energy emitted from the gun is about 70 kev, as determined both by magnetic momentum analysis and time of flight.

3) The average energy of the plasma is about 10 kev.

4) The average number of deuterons accelerated is about 5×10^{16} at 10 cm from the muzzle.

A detailed output energy spectrum was determined in the standard short-barrel geometry at 2 μf and 32 kv. The results as analyzed by time of flight and momentum measurements at a distance of 245 cm from the muzzle are shown in Fig. 2.

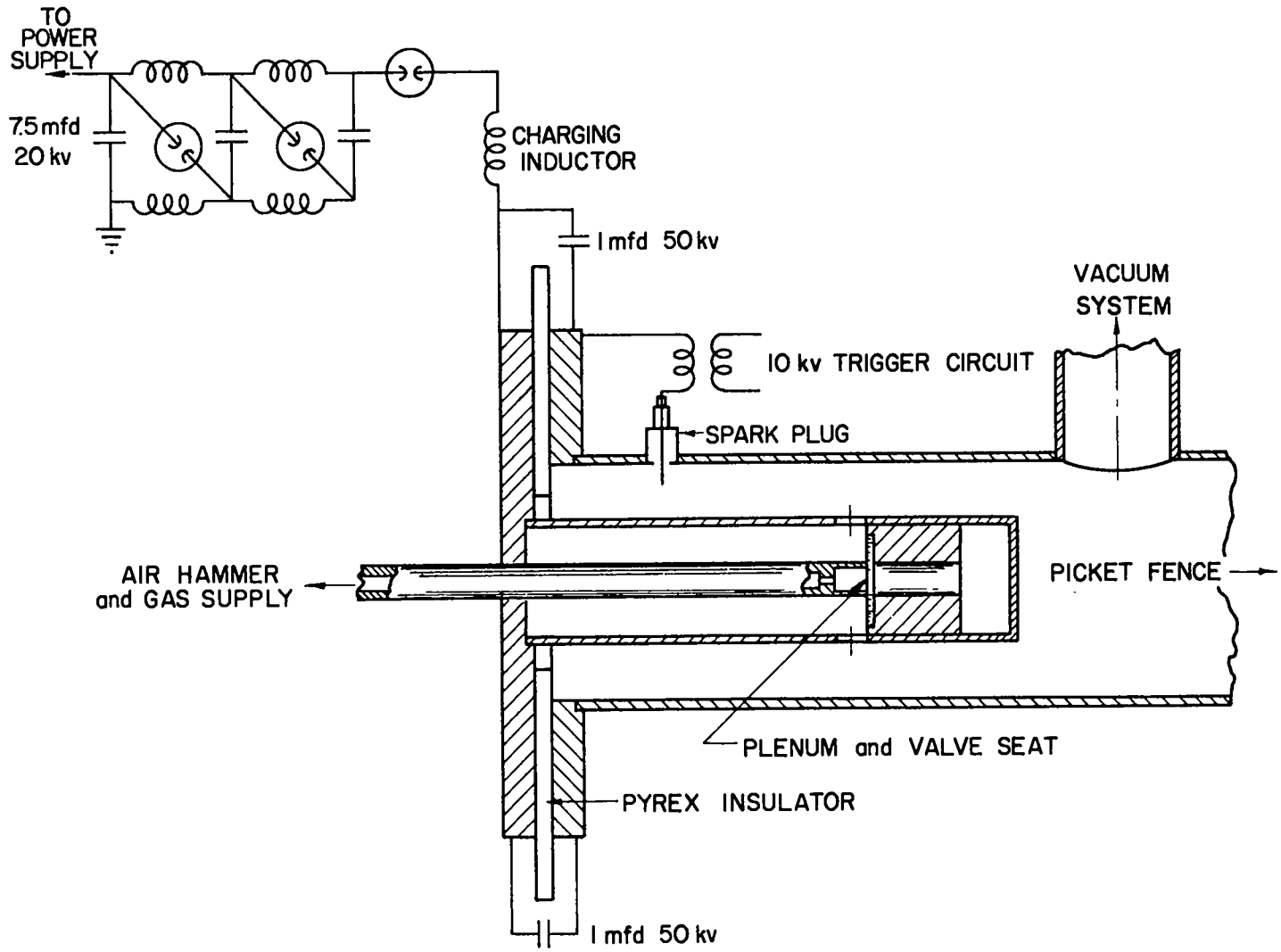

Fig. 1. Hydromagnetic Gun Model III

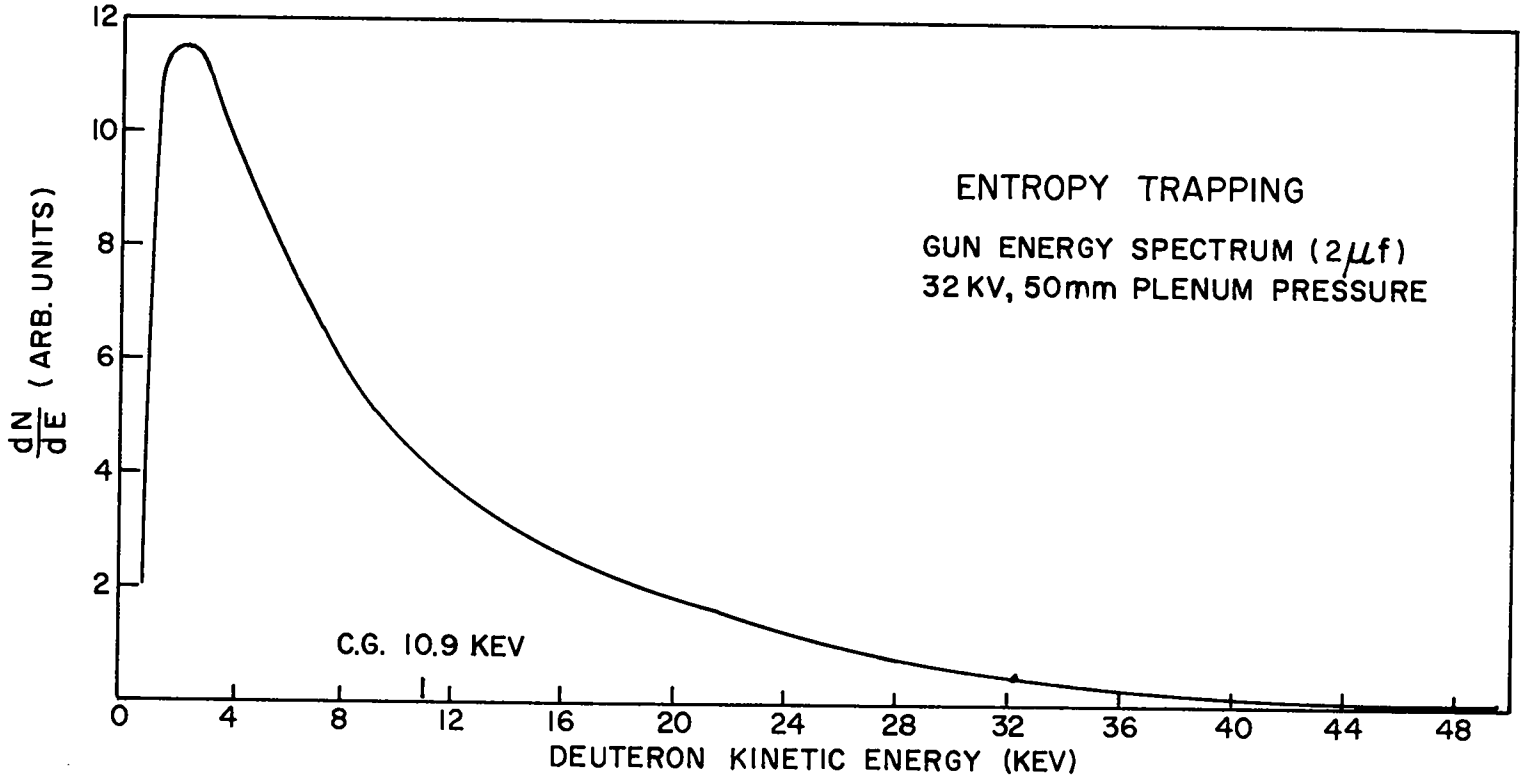

Fig. 2. Energy spectrum of output from hydromagnetic gun

A summary of the performance of the hydromagnetic gun under various conditions is given in Table 1.

Piercing of Plasma Jet at the Entrance Cusp of the Picket Fence

With the plasma gun operating at 20 kv and 150 mm plenum pressure (average ion energy 200 ev) encouraging results have been obtained. The maximum perturbation in the entrance cusp magnetic field for various initial magnetic fields is shown by the curve in Fig. 3. These data indicate that, as the field strength is increased, there is a definite focusing of the plasma stream even in these very low β ($\sim$ 0.1 to 20%) cases. If a similar focusing phenomenon occurs in high-β plasmas it throws doubt on the concept of the critical field, i.e., the density in the plasma stream may increase by focusing so that large magnetic fields may be pierced.

In an effort to clarify the focusing action of the plasma upon entrance to the input cusp of the P.F., time resolved measurements were made with a fast-response (about 1-μsec rise time) thermocouple probe. The element for this probe consisted of 1.4-cm diameter 0.7-mil Cu foil spot welded to a 1-mil Ni wire. The time resolved flux of energy at various radii in the entrance cusp as determined with the probe is shown in Fig. 4. The results were in general agreement with the magnetic field perturbation distribution described above. The spatial distribution of the energy also shows a focusing effect with increased P.F. cusp magnetic field.

An analysis of the plasma at a distance of 160 cm from the muzzle of the gun gave the unexpected result that 60 to 90% of the energetic particles are neutral. This is thought to be due to charge exchange between the energetic positive ions and the gas through which it passes. The long time delay between gas injection and gun firing, together with the confined barrel between the gun muzzle and the P.F., contribute to a substantial gas pressure in front of the gun. By inserting a picket

Table 1. Characteristics of Hydromagnetic Guns

I.D. outer electrode ~ 9.5 cm o.d. inner electrode ~ 5 cm	$C_{\mu f}$	External inductance including header $L_{\mu h}$	Condenser voltage V_{kv}	0.4 cm^3 Plenum P_{mm}	Energy output E_{joules} at 4 in. from muzzle	Number of deuterons N at 4 in. from muzzle	$T_{deut.}$ kev	T_{front} kev	$\frac{N_{charge}}{N_{neutral}}$	Gun length cm, effective	Pulse duration $\Delta t_{\mu sec}$
Original gun	85 (data taken 85 to 14)	0.06	8.7 (Max. V for "clean" operation)	~ 1350 (Min. P for "stable" operation)	~ 225	~ 3.5×10^{19}	~ 0.040	~ 0.2	Not Measured	43	~ 20
Short-barrel gun. Spark plug necessary for breakdown	1.7	~ 0.09	20	50 Gas time delay and pressure show sharp optimum values	~ 32	~ 8×10^{16}	~ 2.5	~ 30	~ 0.5	15	2-5
Short-barrel gun. Gun acts as low pressure deuterium spark gap initiated with spark plug.	2.0	~ 0.019	32	~ 100 Gas time delay and to a lesser extent pressure show sharp optimum values	~ 80	~ 5×10^{16}	~ 10	~ 70	~ 0.1 to 0.5	18	2-5

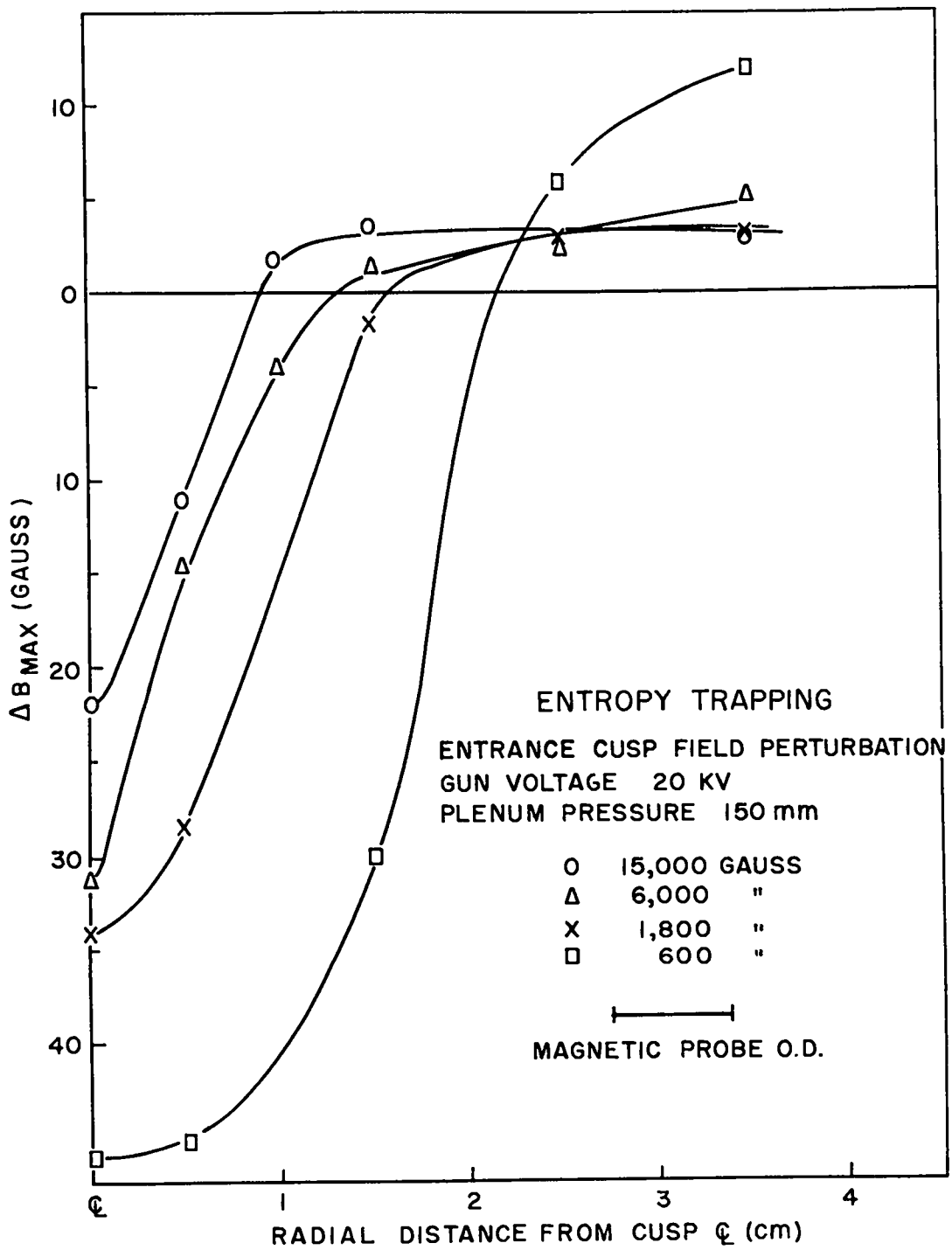

Fig. 3. Entrance cusp field perturbations for various initial magnetic fields

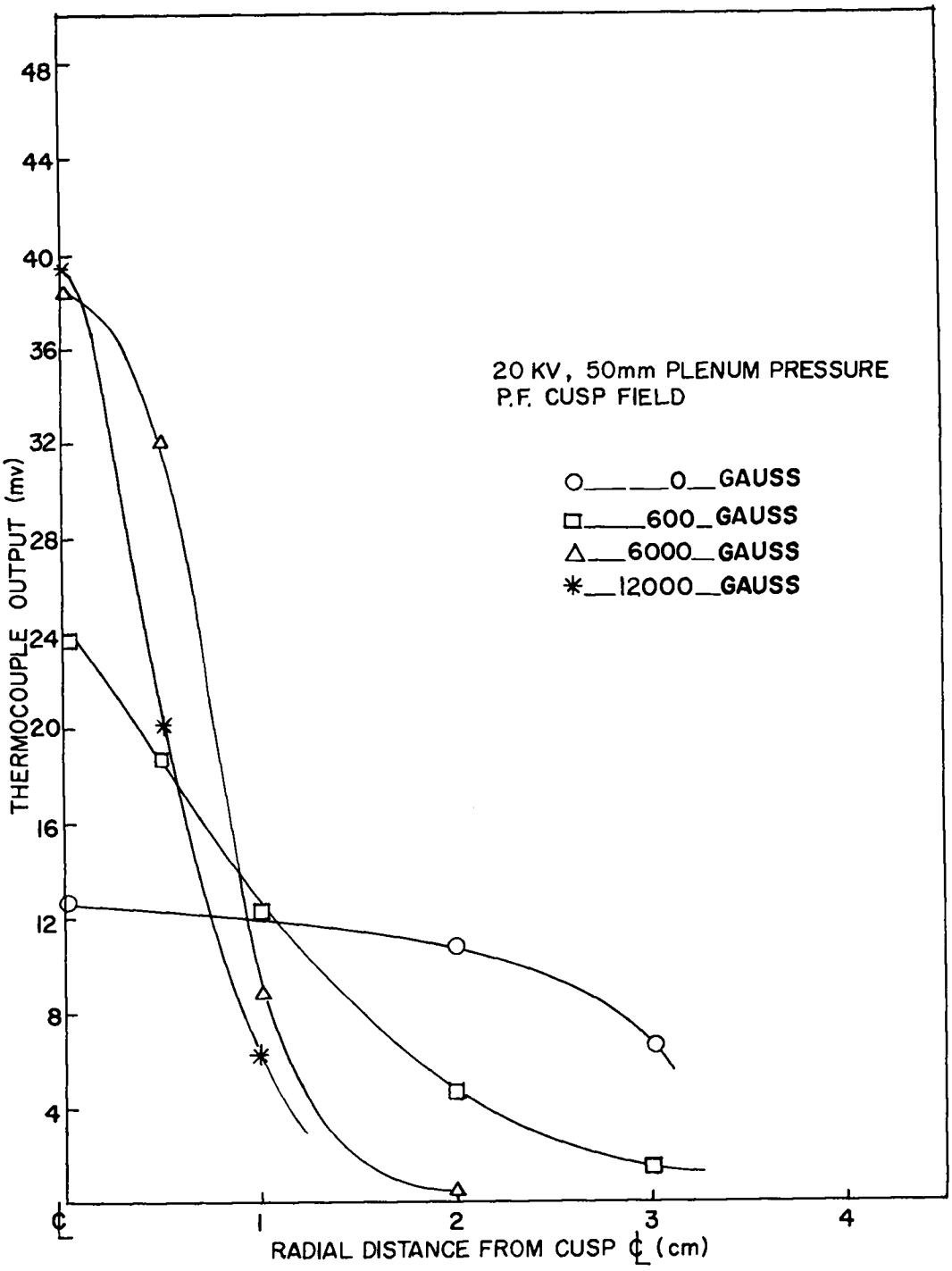

Fig. 4. Radial energy distribution for various initial magnetic fields

fence magnet, which would act as an expansion chamber for this gas, it was hoped that the gas pressure and the neutral component would be reduced. This change in geometry had no measurable effect on the neutral to charge ratio.

Confinement in the Picket Fence

The foregoing data on the entrance cusp show that the magnitude of the perturbation does not decrease with decreasing initial magnetic field. Hence, by lowering the initial field to about 60 gauss it was possible to produce a high β (approximately 1) plasma in the center of the picket fence. The resulting plasma ball had a radius of about 5 cm and a mean lifetime of some 30 μsec. A lifetime of this duration implies confinement since the open time of the entrance cusp is only 2.5 μsec. The mean velocity of the injected plasma was 14 cm/μsec which implies - assuming the trapped ions have this mean velocity and there are no large energy losses during the trapping process - that each ion crosses the ball about 100 times during its lifetime. Thus the particle motion is probably well randomized in direction.

The plasma ball is seriously perturbed by the insertion of a magnetic probe. For example, if a probe is placed outside the ball in the region of compressed field, the signal is changed by the presence of a second probe touching the plasma ball and located 90° around from the first probe. Usually the effect of the second probe on the first is to decrease the amount of field compression seen and to decrease the time duration of the signal. This result, which certainly is expected if all regions of the plasma are connected by the ion motion, precludes the possibility of any complete field mapping in the region of interest.

The diamagnetic effects discussed above were obtained under gun conditions producing low-energy ions. When the gun was adjusted to produce ions of higher energy, it was found that the ions mixed completely with the magnetic field. This phenomenon requires further study.

B. PLASMA GUN

DIAGNOSTICS

A series of experiments has been performed using a magnetic stopping field outside the muzzle of a coaxial plasma gun. Two short solenoids, or Helmholtz coils, were placed coaxially with the gun, and at distances of 12 and 24 cm from the muzzle. These were pulsed, with a rise time of 300 μsec, to fields greater than 10 kilogauss in certain instances. It is easily shown that if such a coil stops a conducting slug which moves into its field, there is a current transient in the coil which is a direct measure of the initial slug kinetic energy. The relationship used is

$$U = \frac{(LI)}{2} \Delta I,$$

where U is the slug energy; LI is the total flux through the coil and remains constant while the slug is being stopped. The kinetic energy of the slug is then easily determined, since L and I can be measured independently. In this experiment, the two coils were driven separately, and the current transients in both were observed. A small transient in the second coil was taken as indicating nearly complete stopping of the plasma by the first.

It was found possible, by the use of sufficiently strong fields, to obtain evidence of efficient first-coil stopping, the indication being a large ratio of coil transients (Fig. 5). However, the plasma energy which went into field energy was an order of magnitude less than that expected if all the gas admitted to the gun were accelerated to the velocity determined by probes. This suggests the presence of a fairly

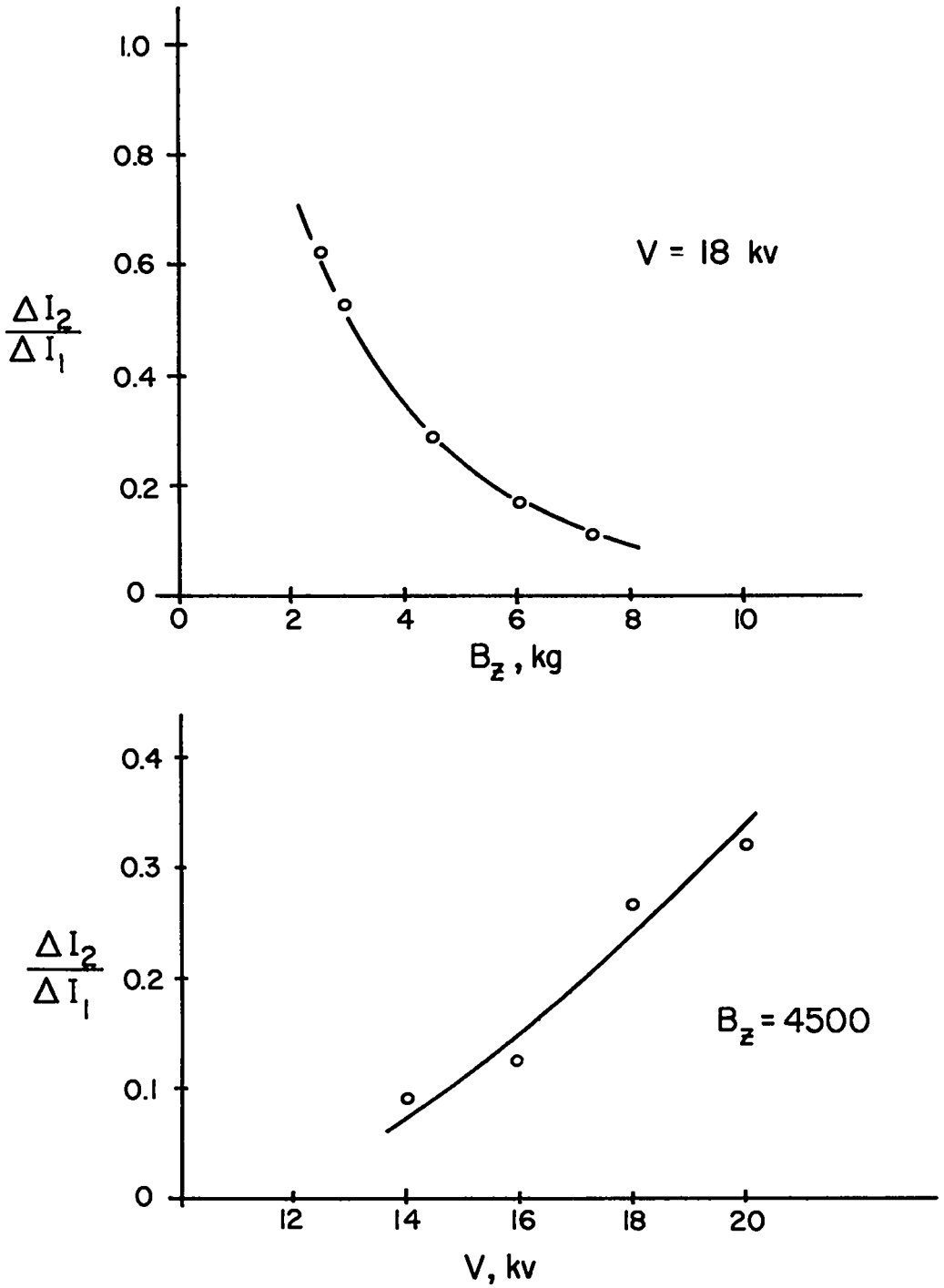

Fig. 5. Ratio of current transients as function of magnetic field strength and gun voltage

large neutral component in the blob, a conclusion which was supported by measurements of a thermocouple plate placed behind the coils. Even when the second coil transient had been made small, indicating good stopping of the charged plasma component, the thermocouple readings remained large.

The gun (input) side of the coil field was mapped by means of magnetic probes during the intrusion of the plasma. It was found that the field was completely excluded from a region around the axis, and whose extension toward the center of the coil depended on maximum field strength in the manner shown in Fig. 6.

A study of oscillations of the plasma left behind in the field when the main field-free component has been expelled leads to the conclusion that the total plasma mass is greater than can be accounted for by the injected deuterium alone. Heavy impurities probably constitute a significant part of the accelerated plasma.

HIGH-VOLTAGE PLASMA GUN

Work is proceeding on the development of a coaxial hydrogmanetic plasma gun which operates at much higher voltages than those used hitherto. The objective is to increase the kinetic energy of the ions from the gun to a level of interest for thermonuclear studies. The output from a standard Scylla-type (80 kv) capacitor bank is fed through appropriate switchgear and an oil-immersed header into a parallel-plate line. This is connected through a pressurized SF_6 chamber to the flanges at the breech of a horizontal coaxial gun. It is probable that a large proportion of the 80 kv of the capacitor bank appears across the gun terminals.

Difficulties in the initial operation of the gun appeared to be associated with the high-impedance load presented by the gun before breakdown, as compared with the low-impedance load of Scylla. The Scylla-type power supply was developed on the basis of the low-impedance load of the Scylla coil, and it did not function properly with the high-impedance load of the plasma gun. The situation has been largely resolved by connecting

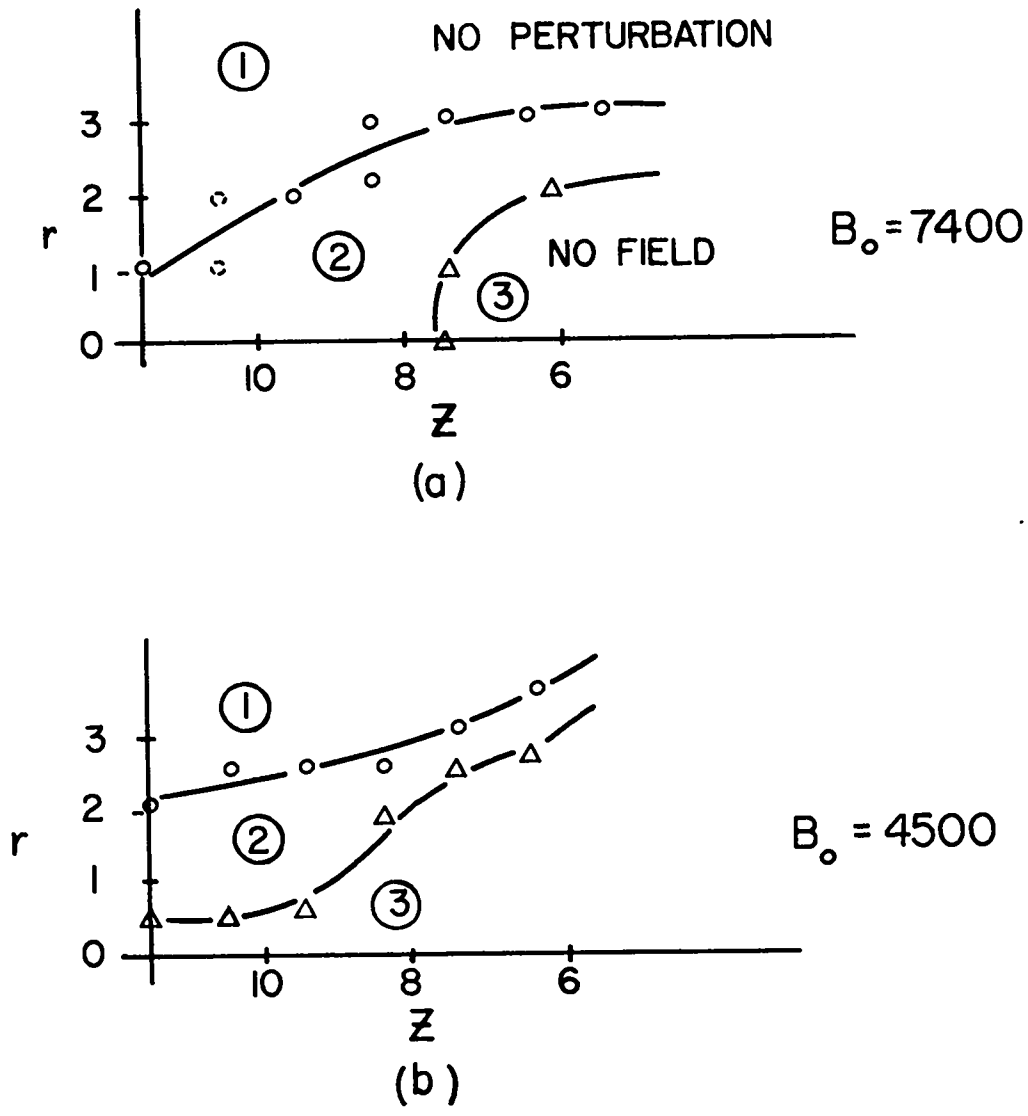

Fig. 6. Coil field during intrustion of plasma

a one-turn coil, having nominally the same inductance as Scylla, in parallel with the gun. In principle, the shunt does not interfere with the operation of the gun, since an inductance is not a dissipative circuit.

Some trouble has also been experienced with the insulator inside the gun. There has been a strong tendency for destructive crowbarring to occur across the surface of the insulator at all times subsequent to the first half-cycle. The insulator has been redesigned and at present consists of a ceramic tube containing two "O" rings in a Teflon insulator; the space between the "O" rings is pressurized with SF_6 in order to minimize crowbarring through the slot separating the ceramic from the Teflon. Even so, there is still occasional crowbarring across the surface of the insulator.

With appropriate delay after gas admission, the gun produces what appears to be a reasonably clear, pink-colored plasma. The energy determined calorimetrically is about 1000 joules, but the observed momentum, from ballistic pendulum measurements, is too high for the approximately 0.5 cm^3-atm of hydrogen gas admitted, moving with a velocity required to account for this energy. In operating the gun, there is still some difficulty, apparently associated with the high voltage, in timing the discharge.

C. SKEW TRAPPING

The skew trapping experiment is designed to test whether or not a beam of energetic deuterons can be injected into a picket fence and be trapped. The cusped magnetic field may be made asymmetric (or skew) by displacing the center line of one set of coils relative to the other, and the angle of the injected beam with respect to the entrance cusp may be varied. Although no rigorous theoretical predictions exist on the feasibility of trapping by this method, the passage of particles through the zero and reverse field on the other side may allow the particle to "forget" its origin and remain trapped for a time determined by losses from the picket fence geometry.

An apparatus has been constructed to examine orbits and confinement times of 30 kev protons in a cusped magnetic field. The magnet consists of 12 pancake coils, each 12 in. i.d. and 24 in. o.d., arranged in two sections of six coils each, 5 in. apart. These two sections are 3 in. off center relative to one another, so as to provide a skew to the picket fence field. The vacuum chamber is 9 in. in diameter at the axial cusp region and 36 in. in diameter in the region of the radial cusp. The measured values of the field in the point cusp and line cusp regions are 12 and 15 kg respectively at an operating voltage of 3 kv on a 24 mf capacitor bank. The half period of the magnetic field is about 45 msec.

For injection into the magnet an R.F. ion source giving proton beams of up to 500 μamp, with about 20% H_2^+ and 10% H_3^+ contamination. The source is operated in a pulsed manner by pulsing the probe voltage in the R.F. bottle.

Measurements have been made thus far on the trajectory of a beam of particles for the first transit through the magnetic field, and a search has been undertaken to determine if any trapping with a significant confinement time associated with it has occurred. The trajectory measurements were made with a movable plate covered with the scintillating material calcium tungstate. The beam was injected at some arbitrary angle across the magnetic field lines external to the first point cusp; the plate was moved axially within the magnet chamber and photographed at each position. It was found that, for a sufficiently high angle of injection, all of the beam could be reflected from the first point cusp and none entered the confinement region. Evaluation of the particle orbits within this region for injection angles just less than the reflection angle have been confused by the angular divergence of the beam, which produces a line on the scintillator plate rather than a point. It is observed that at least some of this beam escapes from the far point cusp after one transit. It is at this time impossible to say whether some of the particles are reflected from the back mirror or not.

The search for a confined component was undertaken using a scintillator-photomultiplier probe which could be positioned within and just outside the confinement region. These measurements are continuing, but so far no evidence for a confinement greater than 20 μsec has been found. As the source pulser does not allow beam shut-off in less than 20 μsec, shorter confinement times have not been investigated.

Work has been initiated on a positioning device to allow injection angles and positions to be changed reproducibly. With this additional equipment it will be possible to start a systematic mapping of the orbits and to investigate confinement times for a known set of initial conditions. Work is also being done on the development of a pulsing system to allow confinement times of less than 20 μsec to be investigated.

D. AXIAL COMPRESSION EXPERIMENTS

PREIONIZED OPERATION OF SCYLLA

Introduction

With the object of transferring the Scylla I operation from the second to the first half-cycle, two preionization schemes have been tried. It has been found that those features of Scylla's operation previously observed during the second half-cycle of the axial field, B_z, can be advanced to the first half-cycle, provided that, in addition to strong preionization, a quasi-static magnetic field B_o is impressed anti-parallel to the direction of B_z during its first half-cycle. The preionization was applied by two methods: (a) an axial discharge between ring electrodes in the wall of the discharge tube and (b) a radiofrequency discharge, either electrodeless or coupled directly through the ring electrodes.

Axial Discharge Preionization

The axial discharge was excited by a 20-kv capacitor (either 1.0 or 7.5 μf) through an ignitron switch to provide gas currents between 10 and 80 kamp. Just prior to applying B_z from the 100-kv bank, the preionizer capacitor was shorted out to remove, as far as possible, the trapped B_o from the plasma. The bias field B_o was excited from a 3-kv, 4800-μf capacitor bank which was coupled to the Scylla coil through an isolating choke. The bias field had a maximum value of 4 kgauss with either polarity. The upper two curves of Fig. 7. present the first half-cycle neutron yield as a function of reversed B_o for two different values of axial preionizer current. Studies of D_β and carbon and oxygen impurity lines show the plasma to be almost completely ionized by the axial discharge.

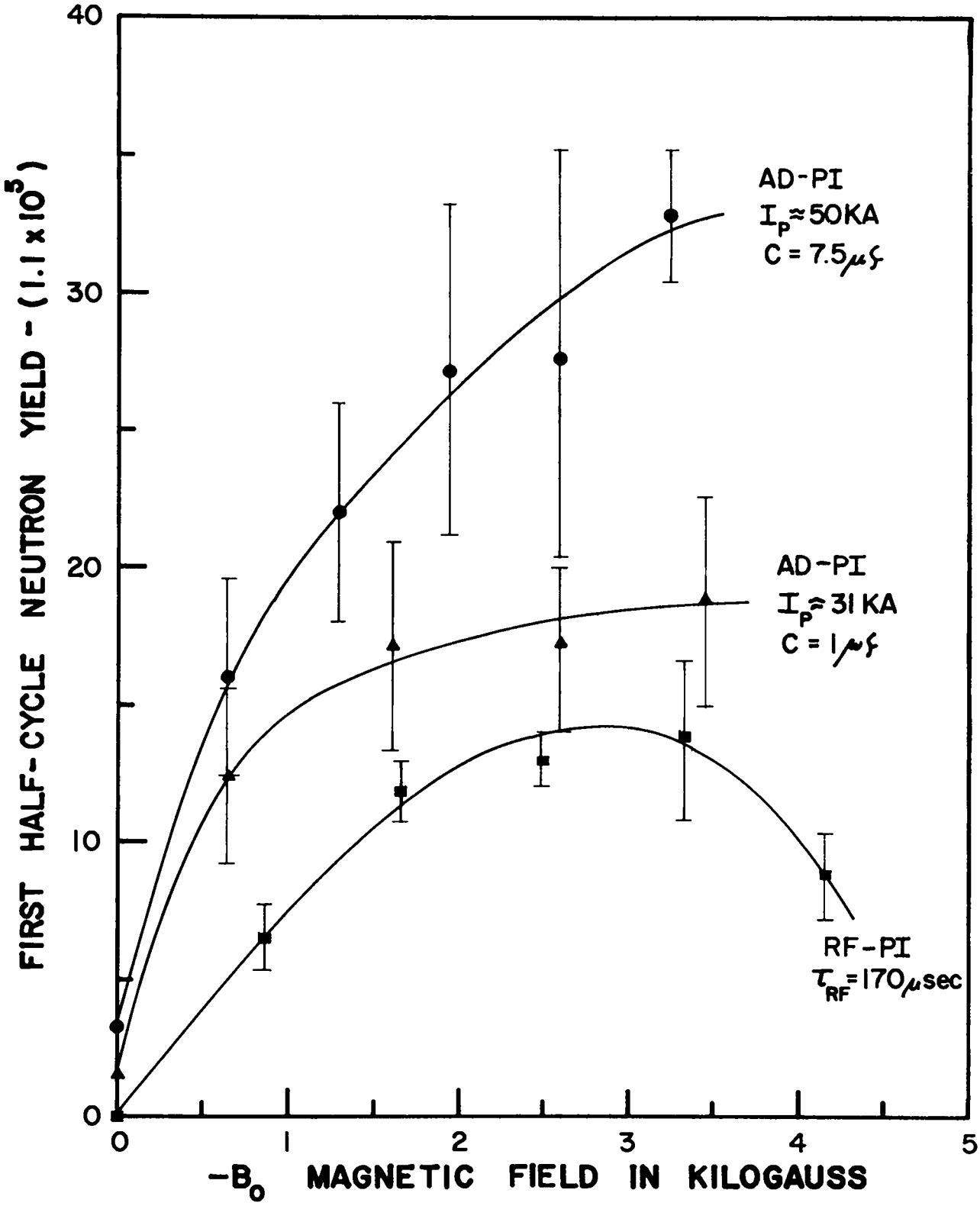

Fig. 7. First half-cycle neutron yields as function of reversed field

Probe signals taken with the probe at the center of the Scylla coil are shown in Fig. 8. For $B_o = 0$, exclusion of the applied B_o from the probe is observed for a small part of the first half-cycle. The diamagnetic effect is intensified by means of reversed B_o (Fig. 8(b)). With positive B_o, i.e., in the same direction as the B_z field, there is no dimagnetism. The spikes on the probe signal correspond to compression of trapped B_o by the initial sheath implosion.

Radiofrequency Preionization

The rf was supplied by a 21-Mc oscillator amplifier whose pulsed 4CX5000A push-pull output stage was capable of 200 kw. However, of the 30 joules supplied to the final plates only about 0.6 joule is coupled to the gas, even with the most efficient scheme used. Studies of the D_β emission confirm that only a small proportion of the deuterium gas is preionized. Nevertheless, when sufficient reversed B_o is applied, neutron emission of the usual second half-cycle time distribution is observed on the first half-cycle. Typical oscillograms are shown in Fig. 9. for the cases in which the rf was coupled capacitively, inductively, and directly through the ring electrodes. The neutron yield as a function of B_o is shown as the lowest curve of Fig. 7.

Streak camera photographs confirm the presence of a plasma sheath implosion at the beginning of the first half-cycle with rf preionization for B_o negative or zero. When B_o is positive, there is no initial implosion.

Conclusions

The requirement of trapped reversed field, in addition to appreciable preionization, for neutron production is definitely established by these experiments. It also appears that the preionization need only be a few percent and that the reverse B_o is responsible for completing the ionization. The fact that no initial plasma implosion or diamagnetism occurs with paralled B_o, strongly suggests that a major effect of reversed B_o is on the initial sheath implosion which precedes the main compression field and the neutron emission.

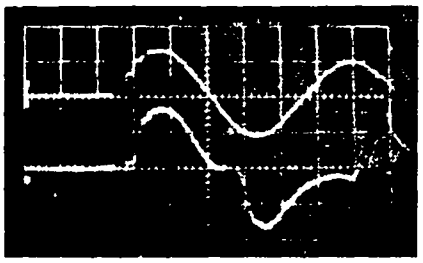

$I_p = 31$ KA ; $B_0 = 0$

PROBE : R = 0 ; Z = 0

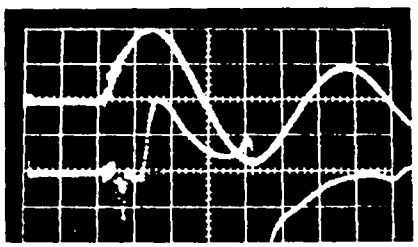

$I_p = 50$ KA ; $B_0 = -4.0$ KG.

PROBE : R = 0 ; Z = 0

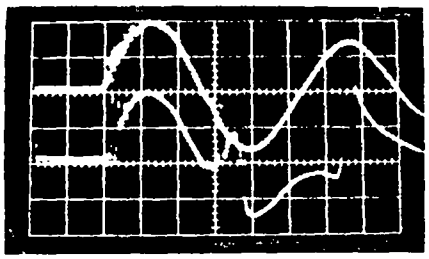

$I_p = 50$ KA ; $B_0 = +4.0$ KG.

PROBE : R = 0 ; Z = 0

Fig. 8. Magnetic probe signals with (a) zero, (b) antiparallel and (c) parallel trapped fields

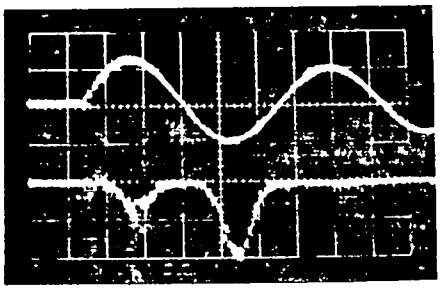

(a)

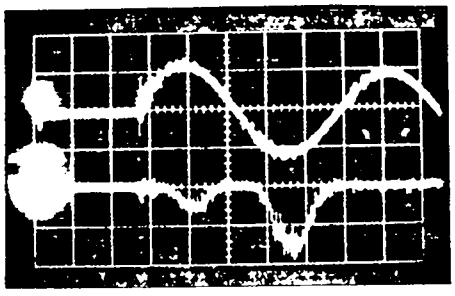

(b)

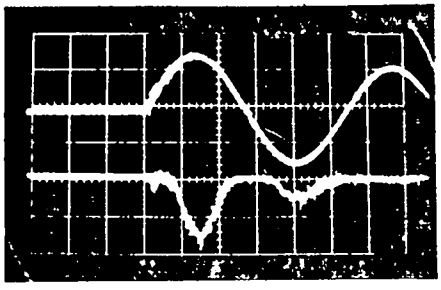

(c)

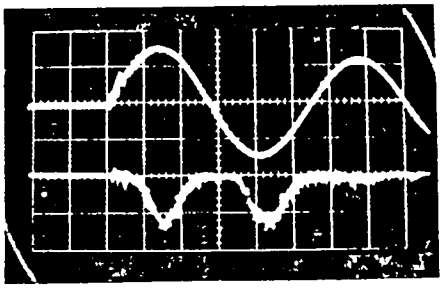

(d)

Fig. 9. Oscillograms of three methods of rf coupling

SCYLLA III

The design of a new version of the Scylla machine has been initiated. It will consist mainly of a bank of thirty 100-kv Tobe capacitors, each switched in the usual way by means of a four-element spark gap. The inductance of the bank will be only 0.013 μh, and so a considerably larger proportion of the voltage will appear across the conventional Scylla coil. With the present coil, the maximum field strength will be increased from 55 to 115 kgauss. Coils of lower inductance may be used if the effect of greater coil lengths and mirror ratios are to be studied. For a coil three times as long as the one now in use, it is anticipated that the azimuthal voltage gradient and maximum magnetic fields will be the same as in the present Scylla II. It is hoped that ion temperatures of 3.3 kev may be attained.

Provision will be made to couple closely to each of the 30 Tobe capacitors the following:

1) Another 100-kv Tobe capacitor to provide a bank of 60 capacitors with an inductance of 0.011 μh. This would give a magnetic field of 169 kgauss and an extrapolated ion temperature of about 4.8 kev. Present voltage and magnetic field conditions would be obtained in a coil four times as long as the one now in use.

2) A set of four or five 20-kev, 4 μh Tobe capacitors. By charging this second bank in parallel with the main bank, but delaying its discharge by means of an added series inductance, it will be possible to achieve switchless power crowbarring. Calculations show that the duration of the coil current can be increased in this manner, although at some sacrifice in the maximum field attained.

ORTHOGONAL PINCH EXPERIMENTS

The so-called orthogonal pinch is a form of axial compression by a time-rising axial magnetic field, similar to that used in Scylla, except that it uses capacitors of lower voltage. The present investigation has been mainly concerned with measurements by magnetic probes of the axial field as

a function of radius and axial position. These have been supplemented by transverse and axial streak photographs at various axial locations. In addition, external loops surrounding the discharge vessel at several axial positions record the time variation of the enclosed magnetic flux. Neutrons, if produced, are detected by a fast photomultiplier-scintillator technique and a silver-activated Geiger counter tube array, with a sensitivity limit of about 6 to 8 x 10^3 neutrons.

The measurements were made primarily in deuterium discharges at pressures of 50 to 250 x 10^{-3} mm mercury in a Pyrex tube shaped to fit approximately the contour of the driving coil (cf. Fig. 10). The aspect ratio (D/L = 0.4) was held fixed throughout. The original coil was 30 cm long and 12.5 cm in diameter, but these dimensions were later both halved, in order to achieve higher central fields for a fixed maximum capacitor energy of 30 kj and 20 kv. The magnetic mirror ratios were varied in the range from 5.0:1 to 1.02:1. The field rise times of 3 to 5 usec were obtained with maximum central fields between 15 and 95 kg.

The internal magnetic probe signals have indicated the following phenomena: (a) Hydromagnetic oscillation of the plasma-field boundary during the first half-cycle; similar oscillations are indicated by the external loops, the amplitudes being largest at the midplane and damping out with distance from this plane. (b) Trapping of the residual first half-cycle field which is compressed in a reversed sense by the rising external magnetic field during the second half-cycle. (c) Apparent intermixing (or annihilation) of the trapped reversed magnetic field.

A plot of the axial field (B_z) versus the radial distance (r) for several axial distances (z) implies that the plasma is initially confined by one or more current layers, but ultimately by a single broad current layer at peak field. Similarly, plots of B_z versus z suggest that the plasma is not restricted to the central region between the mirrors but gradually shifts away from the midplane while the field is increasing.

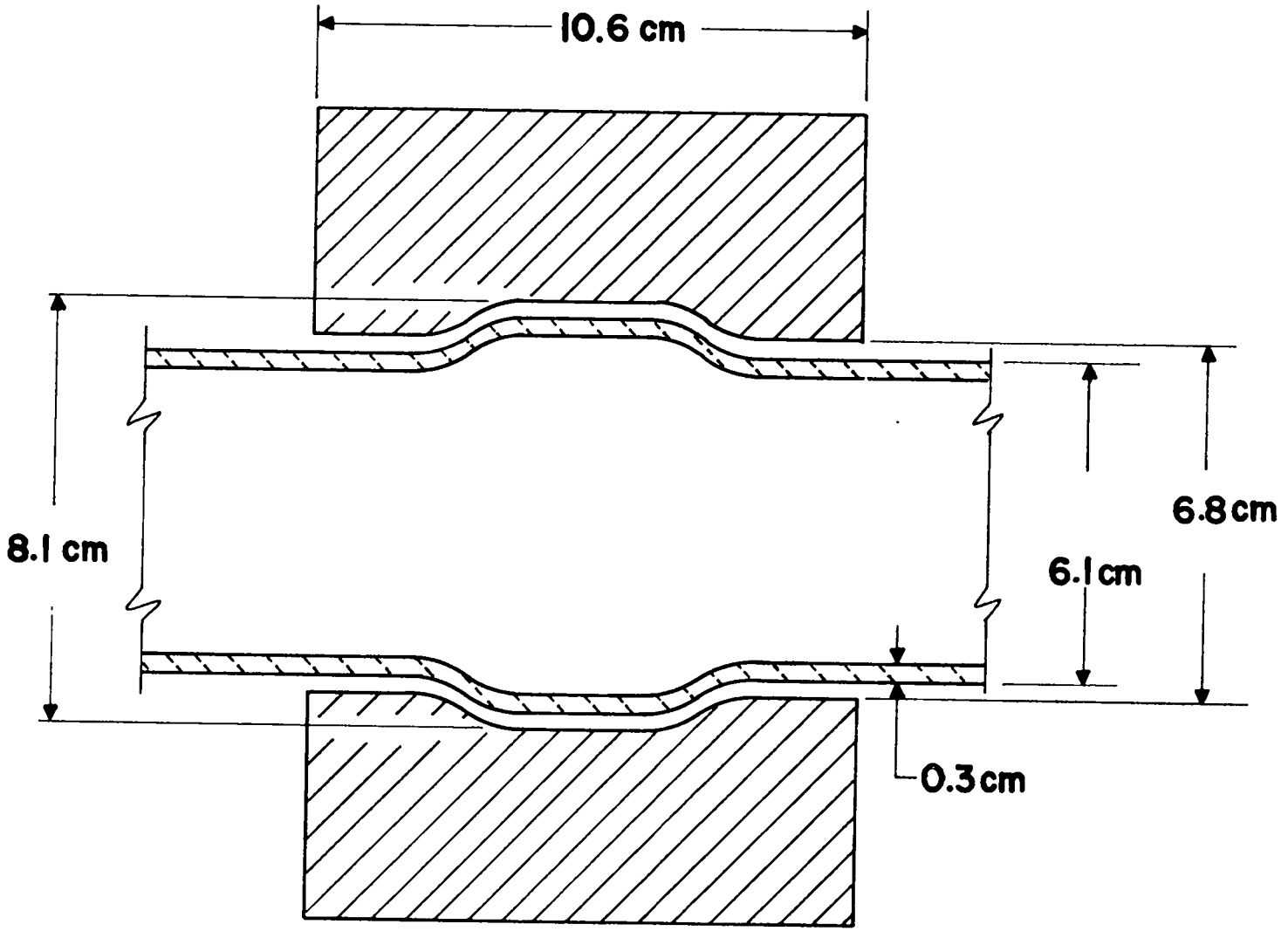

Fig. 10. Shaped tube similar to that used in the orthogonal pinch studies

Streak photographs show the general absence of light at the walls for several cycles. However, at the lowest mirror ratio, i.e., highest central field, the onset of contamination is observed during the fourth and subsequent cycles.

The neutron pulse is centered approximately around the peak field of the second half-cycle, but in some cases a "tail" extends through zero field increasing again in the third half-cycle compression. In other cases, there is a single symmetrical pulse during the second and third half-cycles. The number of neutrons per discharge increases markedly with a decrease in the mirror ratio.

The observations suggest that the deuterium plasma is heated irreversibly by the intermixing of fields. The cause of the decrease in conductivity which permits diffusion of the fields is not known, but it is possible that mixing may result from the radial and axial motions of the plasma, the presence of which is shown by the magnetic probe measurements. Neutron production depends also on initial ionization, which leads to sheath formation, and to reverse fields. Dilution of the plasma caused by streaming through the mirror fields means that there are fewer particles to share the available energy. This could account for the increase in neutron yield with decreasing mirror ratio.

PROPOSAL FOR ZEEMAN MAGNETIC FIELD MEASUREMENTS

Purpose

Attempts to measure the magnetic field in the Scylla plasma by means of conventional magnetic probes have met with only limited success because the probe injects impurities into the hot plasma. The true time history of the magnetic field on the axis in Scylla is thus unknown. The Zeeman splitting of spectral lines in a magnetic field offers a solution, in principle, but in the past the technique has not seriously been developed in Sherwood because the line broadening is in general many times greater than the Zeeman splitting. Recently, it was pointed out that it might be

possible to measure Zeeman splittings even in the presence of large line broadening by taking advantage of the opposite circular polarizations of the Zeeman components when they are viewed along the magnetic field. This technique has been applied successfully to the measurement of solar magnetic fields. In that case magnetic fields of the order of 10 gauss are measured in the presence of line broadening of roughly 1A. Since the Zeeman splitting in the visible for 100 kgauss is ~ 1A, this means that successful results have been obtained for a ratio

$$r = \frac{(\Delta\lambda)\ \text{Zeeman}}{(\Delta\lambda)\ \text{broadening}} \approx 10^{-4} .$$

In Sherwood devices a line broadening of the order of 1-10 A and for 10 kgauss fields approximately 0.1A splitting might be expected; hence r would be 10^{-1} or 10^{-2}. In the case of Scylla absolute accuracy is not as essential as establishing the time symmetry, or lack of it, of the plasma magnetic field about the time of peak magnetic compression. Such measurements would be made by observing optically along the axis of Scylla. In order to localize the measurement to the fireball it is necessary to utilize spectral lines characteristic of the high electron energies present there. Results so far have shown there are two possibilities, namely O VII(λ1630) and N VI(λ1890), which arise from impurities present or easily introduced in small amounts into Scylla. The levels of the ions require electron temperatures of the order of 100 ev for their excitation.

Principle of the Method

The method is to pass the light through a circular polarization analyzer, to disperse it through a spectrograph, and finally to view the broadened spectral line by means of two slits, S_1 and S_2, as illustrated in Fig. 11. A null method is applied in which the difference in the intensities I_1 and I_2 of the two slits is measured. Thus when the two slits are symmetrically spaced on the wings of the line, there is no signal in the absence of magnetic field or of the polarizer. When there is a magnetic

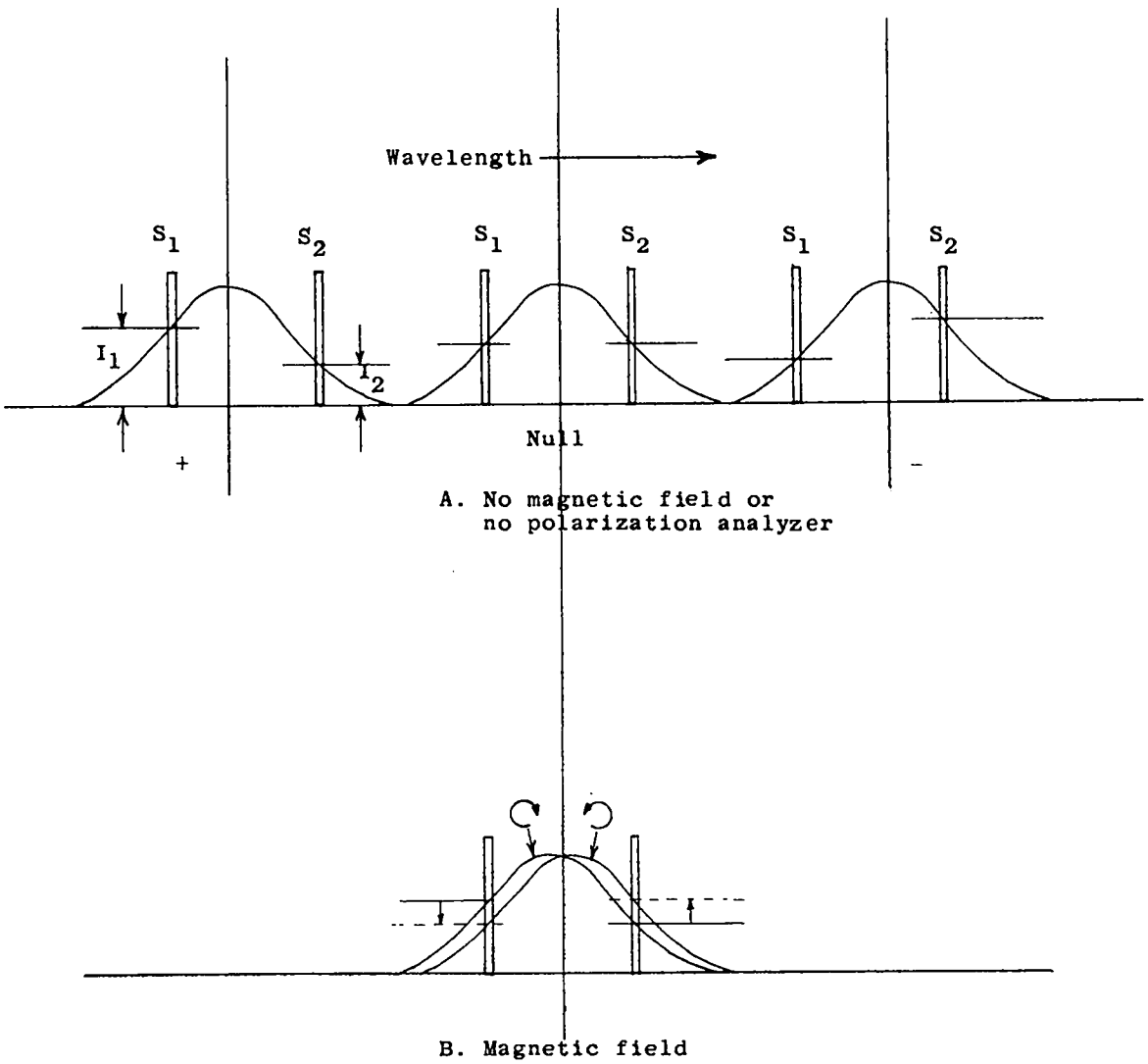

Fig. 11. Principle of Zeeman magnetic field measurements

field, and polarization analyzer as in the case of Fig. 11B, the difference signal is positive or negative according as the analyzer is set for right-handed or left-handed polarization.

In the solar magnetic field studies the polarization analyzer is modulated at 120 cps to detect alternately l-h and r-h polarization so that the alternating difference signal is proportional to the magnetic field. In the case of Scylla such modulation would have to be at about 10 mc. The electro-optic DNP retardation plate used in the solar work to accomplish modulation at 120 cps may conceivably be satisfactory at 10 mc, but the shortest wavelength of its pass band is about 3600A. Therefore it can be employed only in the visible region. At present the usable spectral lines from Scylla appear to lie in the vacuum ultraviolet, requiring quartz and fluorite optics for which modulation techniques are not readily available. It is therefore proposed to perform the initial experiments unmodulated in the near vacuum ultraviolet.

Apparatus

The apparatus to be used is shown in Fig. 12. The circular polarization analyzer consists of the combination of the Babinet-Soleil compensator and the Rochon analyzing prism. The former is a variable quarter wave plate to shift the phases of the two linear degrees of polarization coincidence for l-h polarization and out of coincidence for r-h polarization. The resulting linearly polarized light is analyzed by the Rochon prism. The deviated extraordinary ray from the Rochon prism polarized at right angles to the paper is shown by the dashed line, and the solid lines indicate the optical path of the ordinary ray, linearly polarized in the plane of the paper. Since calcite cuts off at about 2100 A, quartz must be used for the circular analyzer. This has a low wavelength limit of about 1800 A and therefore the observations will be limited to the N VI line until other lines are discovered.

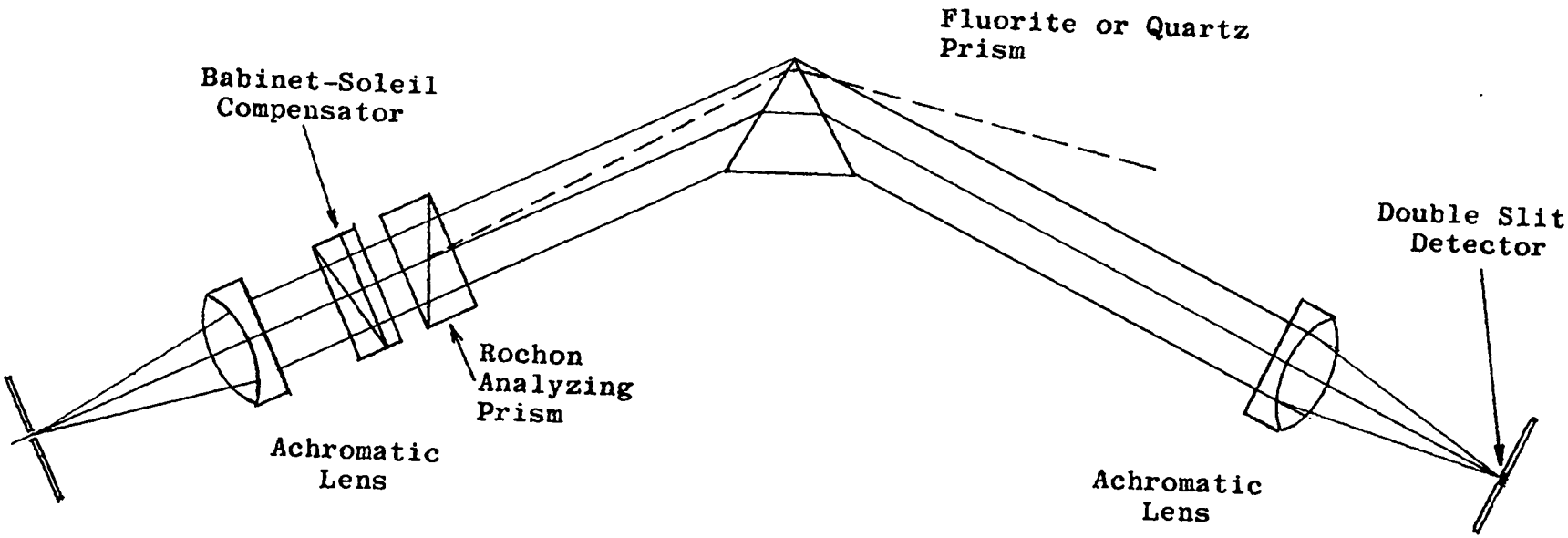

Fig. 12. Proposed apparatus for Zeeman measurements

Both fluorite and quartz are quite dispersive in this wavelength region. Fluorite has a low-wavelength cutoff at 1250 A but only about half the dispersion of quartz. At 1850 A a 4-cm prism of quartz has a dispersion of 2.8 A/mm for a 1-meter arm and a resolving power of about 20,000. Fluorite has a dispersion of 6.1 A/mm and a resolving power of about 11,000. The line shape attainable with a prism spectrograph should be good, while that of the Seya-Namioka vacuum grating spectrograph is quite asymmetric.

E. PERHAPSATRON S-5

Research on the stabilized toroidal pinch has been continued with the construction and operation of the largest in a series of toroidal pinch machines, Perhapsatron S-5. It has a major radius of 64.6 cm and a minor radius of 13.3 cm.

Perhapsatron S-4 exhibited a catastrophic radiation energy loss in the vacuum ultraviolet region (100 to 1200 A) of approximately 1000 joules/μsec starting early in the discharge cycle prior to the first current maximum. In the initial operation of Perhapsatron S-5, it was found that, as in PS-4, there was an energy loss in the vacuum ultraviolet amounting to approximately 500 to 1000 joules/μsec. The radiation loss in PS-5 differed, however, from that in PS-4 in the respect that the onset time could be delayed beyond the first half-cycle of the discharge by decreasing the deuterium pressure to 5×10^{-3} mm at a base pressure of 7×10^{-7} mm Hg. Since the behavior of the first half-cycle of the discharge is of paramount importance to the operation of the machine, the absence of the main (ultraviolet radiation) energy loss was considered encouraging. The characteristics of the machine operation under which the ultraviolet radiation data were taken are summarized in Table 2, line A. The results of ion temperature measurements, under these conditions on the 4686 A line of ionized helium are summarized in Fig. 13. It is of interest to note that an apparent temperature increase accompanied the improved operating base pressure. This is in accord with the delay in the onset time of ultraviolet radiation emission being the result of clean or discharge condition.

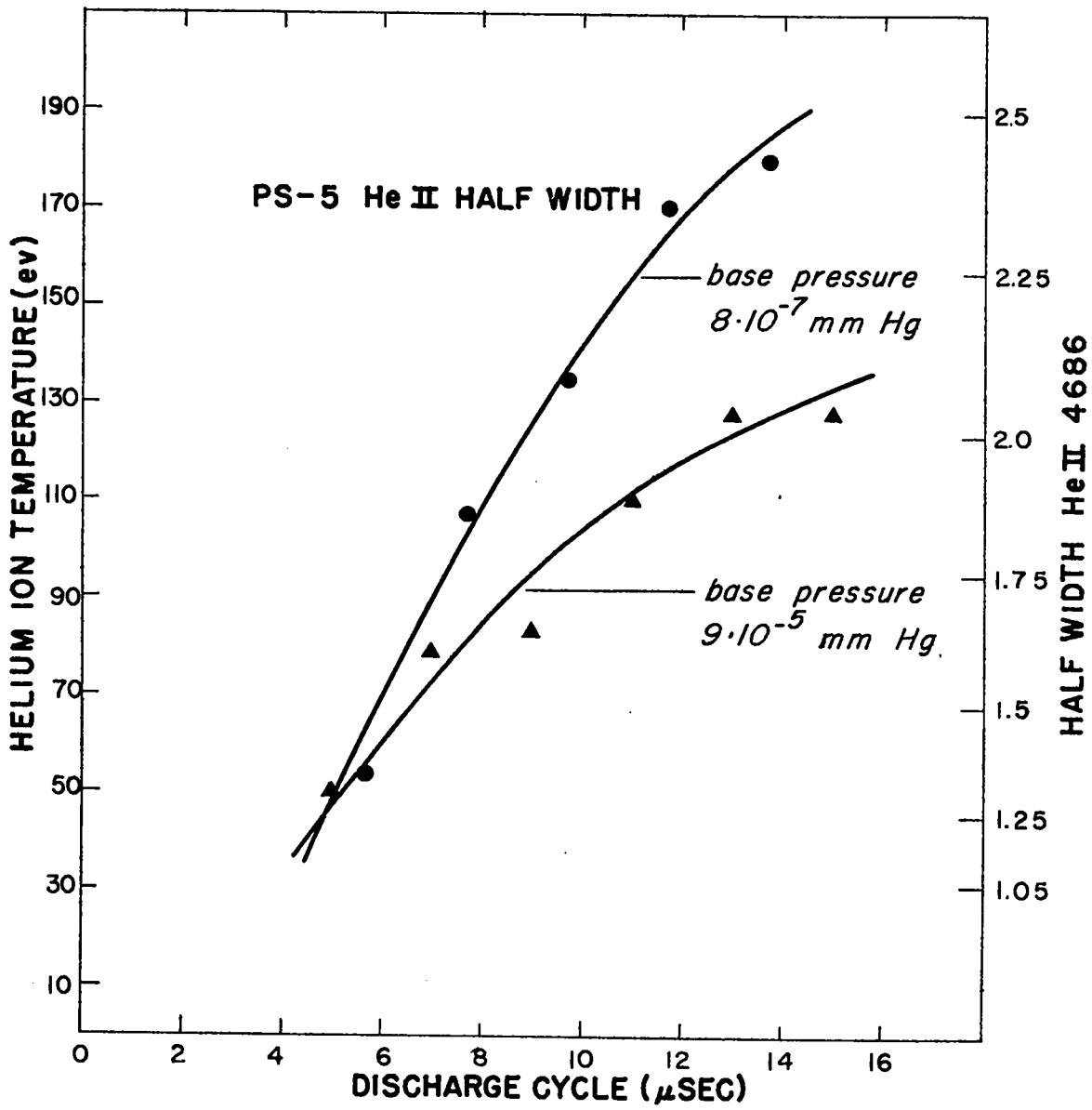

Fig. 13. Ion temperatures in Perhapsatron S-5

Table 2

Condition	Condenser Bank, 10^6 Joules at 20 kv	Bank Voltage, kv	Peak Current, 10^3 amp	Discharge Period, μsec	Stabilizing B_z Field, gauss
A	0.18	13	257	47	1070
B	0.36	13	360	66	1500
C	1.12	20	940	125	3910

The characteristics of PS-5 operating with the capacitor banks doubled in capacitance are summarized in Table 2, line B. A maximum yield of 10^8 neutrons/burst was observed under these conditions. If of thermonuclear origin, this would indicate a gas temperature of approximately 720 ev. By evaluating the integral $\int_0^{T/4} I^2 R dt$, using a value of 20 milliohms for the discharge resistance, a value of ~ 800 ev is obtained for the temperature of the discharge.

A question naturally arises at this point as to why the resistance of the discharge remains so high (20 milliohms) at a temperature of hundreds of electron volts. Conversely, if the energy loss mechanism of the discharge has indeed been disposed of, will the gas not rise to the aforementioned temperatures through the process of ohmic heating.

To answer these and other allied questions arising from past research on the stabilized toroidal pinch, PS-5 has been connected to the Zeus condenser bank. Expected discharge conditions for PS-5, Zeus are summarized in Table 2, line C. The experimental arrangement is shown in Fig.14. The Zeus bank has already been fired into PS-5 at 370,000 amp, and progress is being made toward operation at higher voltages.

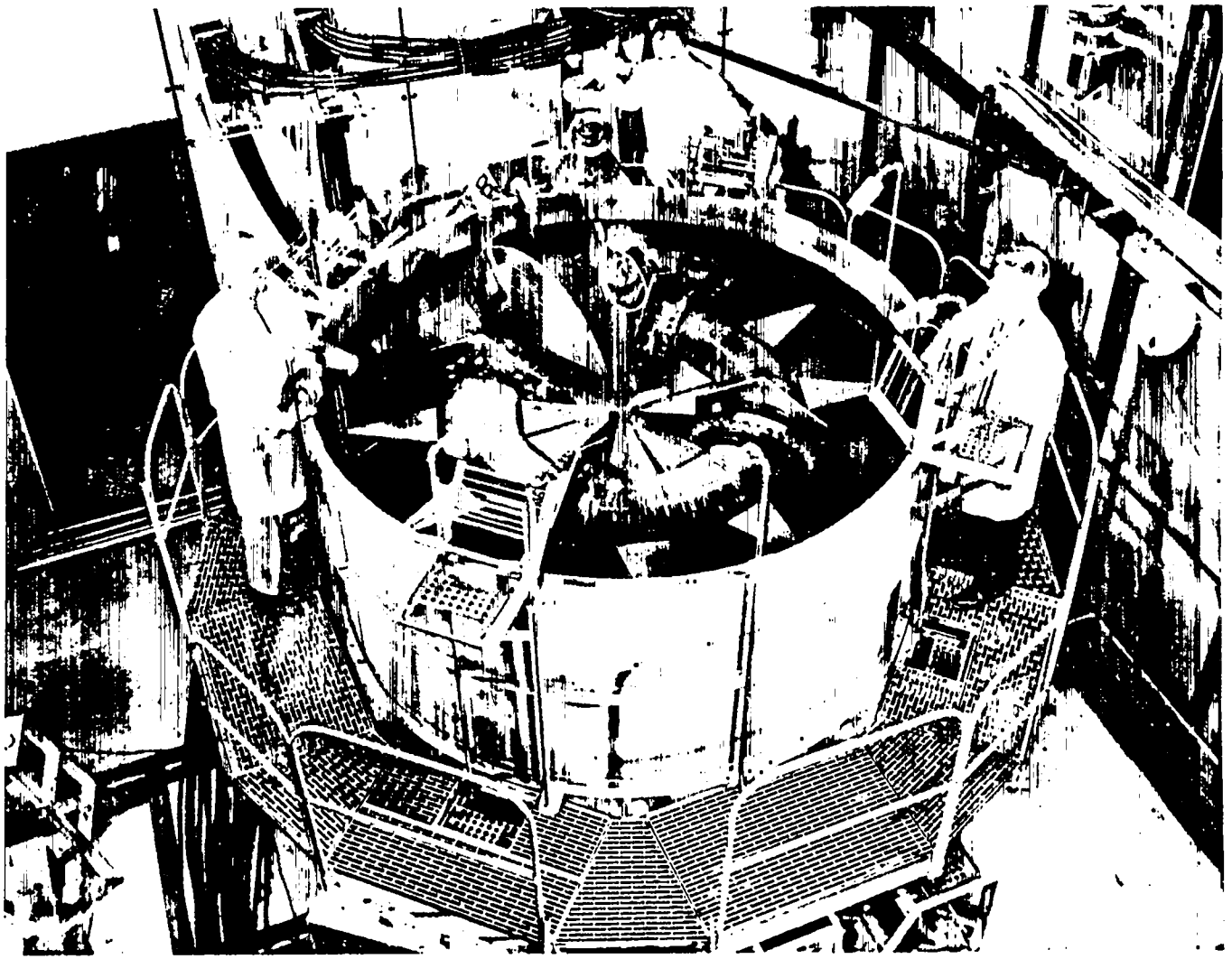

Fig. 14. Perhapsatron S-5 connected to Zeus capacitor bank

F. IXION

VOLTAGE LIMITING EXPERIMENTS

Introduction

It has been observed that the ion energy of Ixion is limited by the fact that the voltage between the center and outer electrodes (back emf) cannot be made to exceed about 8 kv. A two-step boost experiment has been performed in an attempt to force the voltage higher. The plasma is set into rotation in the usual way, using a capacitor bank charged to 7 kv. Then, after the plasma rotation is well established, the first bank is disconnected and a second bank, the boost bank, is switched on in its place. All the data to be presented here were taken with a series 1.33-ohm resistor in the second bank circuit. Even with boost bank voltages as great as 20 kv, the peak Ixion voltage regulates itself and never exceeds 8 kv.

Distribution of Current During Boosting

To study the role of the end insulators in the effects just described, an experiment was performed to determine if radial currents were flowing across the insulator surfaces. An internal current loop, which measures the total current threading it, was installed on each insulator. By comparing the indicated current with the total electrode current measured externally, it is possible to determine what radial current, if any, flows in the gap between the loop and the insulator. Sample results of the experiment are shown in Fig. 15. The top trace is the time integrated signal of the internal loop giving the current which threads

INTERNAL LOOP EXPERIMENT

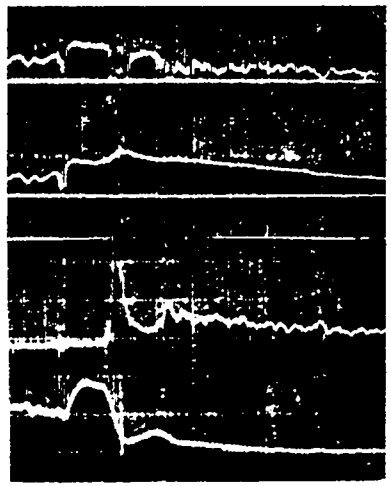

20 μsec/cm (DELAYED TRIGGER)

B_0 = 9.4 KG

Fig. 15. Oscillograms in Ixion boosting experiment

it. The second trace shows the total current supplied to the corresponding electrode. The third trace is the difference of the first two and shows the time history of the current flowing across the insulator. The bottom trace is the Ixion voltage. The time of switching the boost bank is t_2. From traces such as these as well as from magnetic probe data the following conclusions can be drawn:

1) There are no insulator currents during normal operation with low boost voltages.

2) The peak voltage attained is not controlled by insulator conduction.

3) The abrupt drop of voltage and increase of electrode current at the later time t_3 is a result of the onset of insulator currents. The sharp spike of insulator current at the time t_3 is attributed to the discharge of a part of the previously established rotating energy when the voltage drops as a result of the sudden breakdown in the insulator region.

Dependence of Voltage Limiting Upon Magnetic Field

The dependence of peak voltage was investigated as a function of magnetic field. The results appear in Fig. 16 , in which the abscissa is the boost bank initial voltage and the ordinate is the corresponding peak Ixion voltage attained. Each curve was obtained with a different value of applied magnetic field B_o (as measured in vacuum at the midplane). Two effects are immediately apparent:

1) The machine has a strong voltage saturation.

2) The limiting voltage depends strongly upon the value of magnetic field.

Role of Ion-Neutral Collisions

It is suggested that the voltage limiting phenomenon is produced by ion-neutral interactions. When a drifting charged particle collides with a neutral, it will on the average lose a portion of its drift energy. As a result, the ion will fall in the electric field, gaining energy until it has resumed its proper drift motion. The overall effect is that the

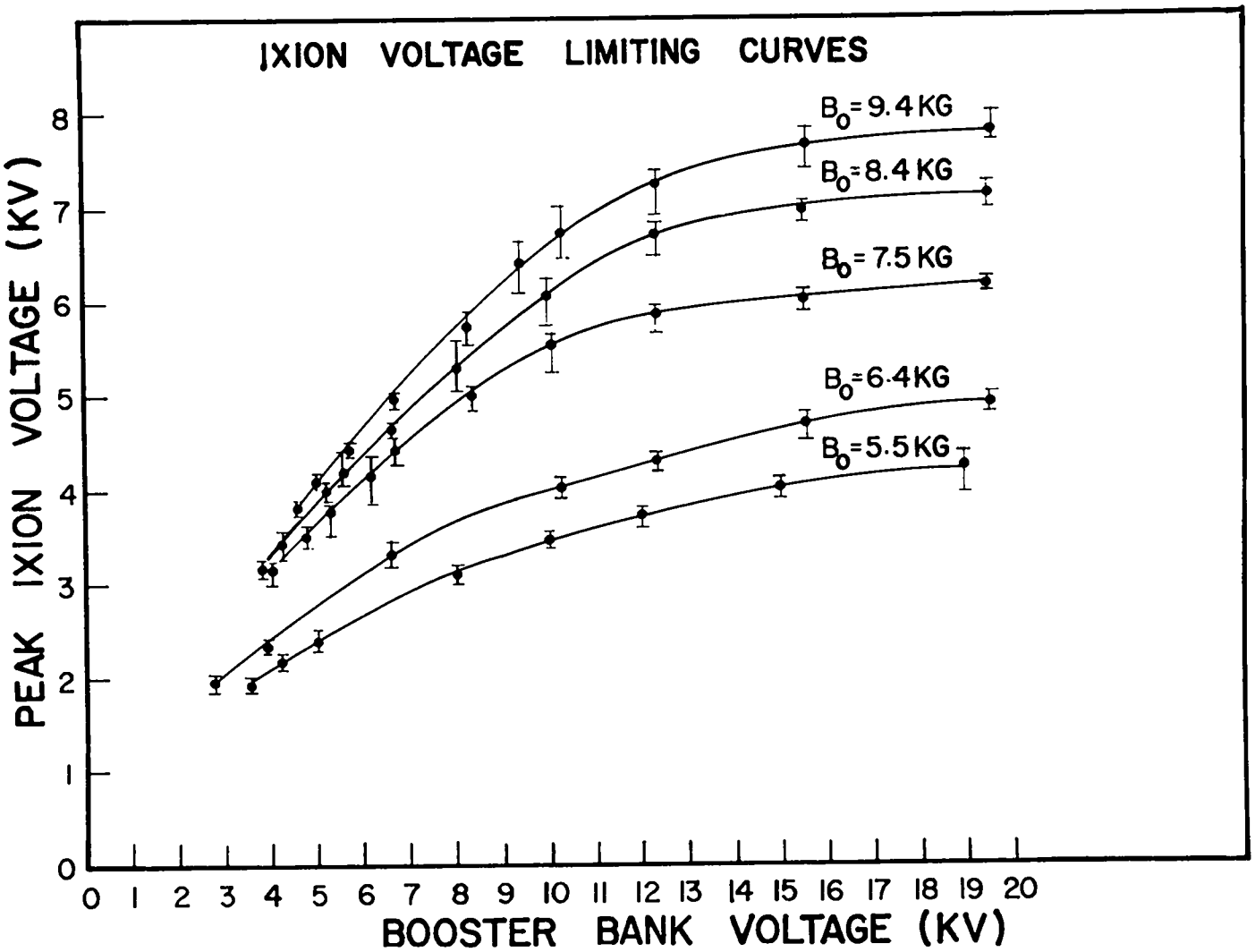

Fig. 16. Peak Ixion voltage versus boosting voltage for various magnetic fields

neutral gas background exerts a viscous drag on the rotating plasma. This energy loss manifests itself as a lowered Ixion resistance. The ion-neutral energy loss rate depends on velocity through the collision rate factor $\langle\sigma v\rangle$ and the average ion energy loss per collision. Since the drift velocity depends on both the magnetic and electric fields, the ion-neutral interaction can account for the velocity dependence of Ixion resistance on both voltage and magnetic field.

If the collision cross section is a rising function of velocity, the resulting nonlinear Ixion resistance will produce voltage saturation effects such as are observed. The Ixion resistance to be expected from ion-neutral interactions can be obtained from first-order drift theory and dimensional arguments. The result is

$$R = k\frac{B^2}{\langle\sigma v\rangle} \quad , \tag{1}$$

where k depends on Ixion geometry, neutral density n_o, ion density n_i, and ion mass m_i. An average cross section $\bar{\sigma}$ and average relative velocity $\bar{v}$ are defined, so that $\overline{\sigma v} = \langle\sigma v\rangle$. Letting v be proportional to the drift velocity, i.e., $v \propto V/B$, it is found that

$$\bar{\sigma} \sim \frac{B^3}{RV} \quad , \tag{2}$$

where V is the Ixion voltage. This gives the average cross section as a function of Ixion voltage. The results obtained from this formula normalized to a magnetic field $B_1 = 7.5$ kgauss are given in Fig. 17. The average cross sections deduced from the data by means of Eq. (2) are plotted against the average normalized velocity $V/(B/B_1)$. Each curve represents a cross section derived from data obtained with a different magnetic field strength. Ideally, if the theory is correct, all the curves should be identical. The fact that they do not exactly coincide could be explained by experimental errors and slight differences in machine operation at different magnetic field values.

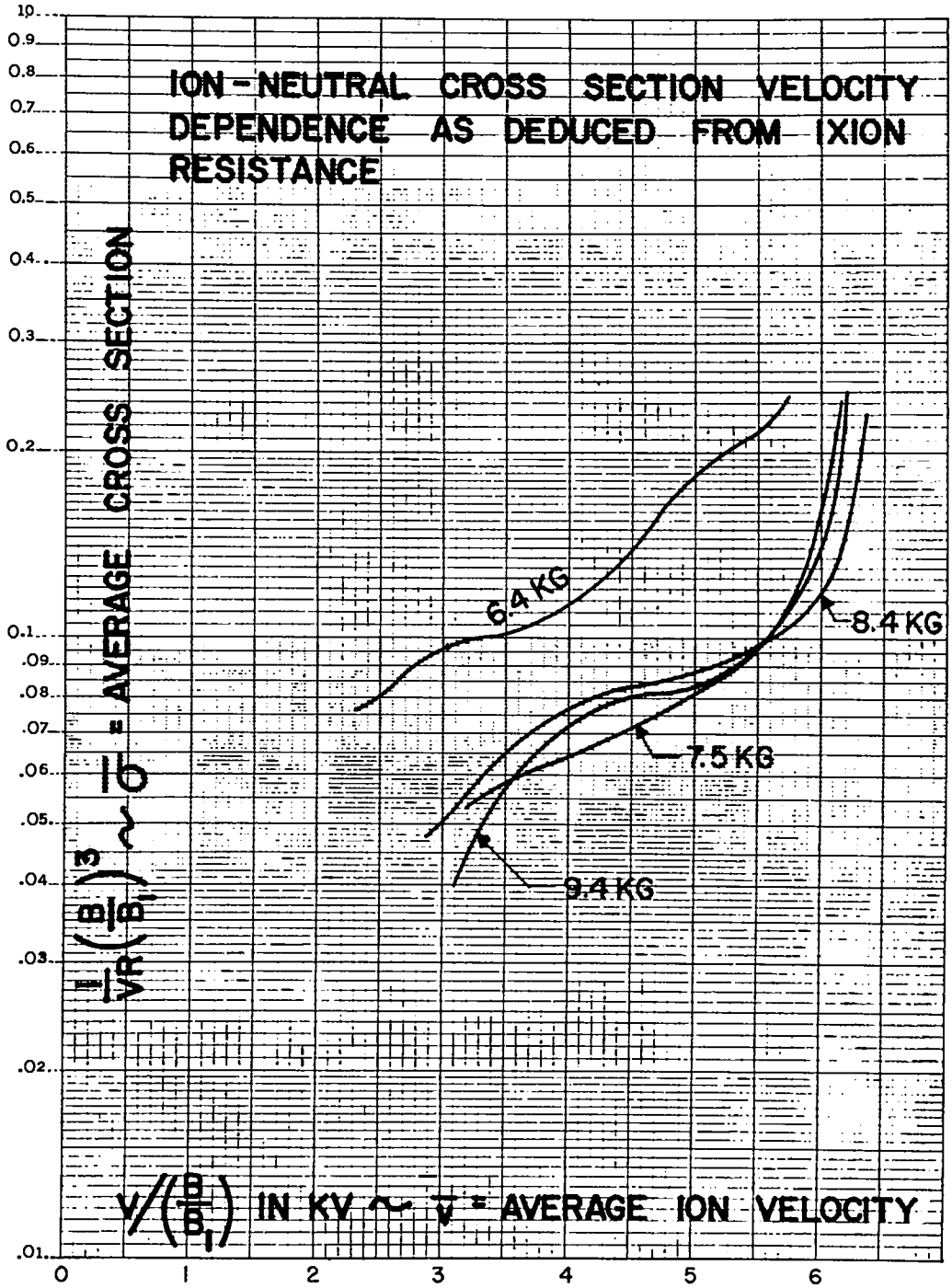

Fig. 17. Ion-neutral interaction cross sections derived from Ixion resistance

Examination of Fig. 17 shows that the equivalent cross section has a steep rise at some limiting drift velocity which is roughly the same for all values of voltage and magnetic field. This suggests that the voltage limiting phenomenon occurs when the ion drift velocity reaches the threshold of an inelastic process having a high cross section.

In conclusion it can be stated that, although there seem to be insulator problems, the voltage limiting is a more basic gas phenomenon.

G. SCATTERING OF MICROWAVES BY AN IONIZED GAS

The object of this experiment is to measure the intensity, frequency spectrum, and angular distribution of microwaves scattered by an ionized gas. It is known from theory that this phenomenon is directly related to the fluctuations in the dielectric permeability of the gas. In the case of a cold plasma these fluctuations are proportional to the density fluctuations in the medium; thus

$$I \propto |\delta n_{(\underset{\sim}{k}-\underset{\sim}{k}_o)}|^2 ,$$

where I = the intensity of scattered light,

$$\delta n_{\underset{\sim}{k}} = \int e^{i\underset{\sim}{k}\cdot\underset{\sim}{r}} \left[n(r,t) - n_o(r) \right] d^3\underset{\sim}{r}$$

= Fourier component of the deviation of electron density about its mean value, n_o.

$\underset{\sim}{k}$ = wave vector associated with scattered light

$\underset{\sim}{k}_o$ = wave vector associated with primary light

Calculations of $|\delta n_k|^2$ for a plasma of electrons and heavy smeared-out ions in thermal equilibrium give the result

$$|\delta n_k|^2 = n_o V \left[\frac{k^2\lambda_D^2}{k^2\lambda_D^2 + 1} \right] ,$$

where λ_D is the Debye radius and V is the volume involved in the scattering process. This formula shows that independent scattering from electrons can occur only for wavelengths such that $k\lambda_D > 1$. The process is, therefore, unimportant for all attainable microwave frequencies and typical laboratory plasma. In the opposite limit, $k\lambda_D \ll 1$, microwave scattering is possible, but is reduced by the factor $(k\lambda_D)^2$ due to the Coulomb interaction which manifests itself in the collective plasma oscillation modes of the medium. Moreover, the scattered radiation will be incoherent with respect to the primary unscattered radiation since the collective modes oscillate with the characteristic plasma frequency ω_p. As a result, it is to be expected that the frequency ω of scattered radiation is altered from the frequency ω_o of the primary radiation. Calculations show that

$$\omega = \omega_o \pm \omega_p .$$

Under conditions of thermal equilibrium the "collective" scattering cross section per unit volume is given by

$$\sigma \approx 4\, n_o \left(\frac{e^2}{mc^2}\right)^2 \left(k_o \lambda_D\right)^2 \psi ,$$

where $k_o = \omega_o/c$ and ψ is a function whose value lies between 2 and 3 for widely varying plasma conditions.

In the experimental arrangement, the total scattering volume consists of a R.F.-excited glass bottle with a scattering volume of approximately 4×10^4 cm^3. The primary energy is provided by a 200 watt C.W. tuneable 10-cm magnetron and amounts of about 1/8 watt/cm^2 over an effective plasma area of 1600 cm^2. For a plasma density of 10^{10} electrons/cm^3 and an electron temperature of 10 ev, the total energy scattering rate would be about 6×10^{-15} watt. Solid angle considerations associated with the detector will reduce this quantity to 10^{-17} watt. The most sensitive microwave radiometer, constructed during the past months, has a sensitivity of about 10^{-15} watt, and thus is incapable of detecting

radiation scattered from electron plasma oscillations in thermal equilibrium. Its main application is therefore restricted to plasma configurations which are unstable or sufficiently near instability to increase $|\delta n_k|^2$ by several orders of magnitude above its equilibrium value.

Preliminary measurements have shown that the noise spectrum of the high-power magnetron oscillator is sufficiently broad and intense to mask the scattered radiation entirely. Efforts in the immediate future will therefore be directed towards the achievement of a stabilized high-power source of radiation.

H. CALCULATION OF IONIZATION PROBABILITIES IN A PLASMA

The large radiation losses from impurities in hydrogen discharges has made it desirable to calculate the energy radiated from the ionized states of impurity atoms. With the results it may then be possible to determine the electron temperature and percentage of impurities as a function of time.

In the calculations of the probability of ionization of an atom by electron collisions in a plasma, it is necessary to evaluate Slater integrals. These are infinite double integrals involving the product of four radial wave functions, three of which are for states in the continuum of positive energy. The integrals cannot be evaluated as they stand, because the free electron wave functions oscillate indefinitely. Attempts to resolve the integral into computable multiple series have not been successful because of divergences, and so a different procedure has been developed.

The free-state wave functions are confluent hypergeometric functions, which can be represented by a Mellin-Barnes integral. The Slater integral then becomes a five-fold integral involving gamma functions of complex variables and three complex parameters as exponents. One integration, with respect to radius, can be carried out as a known Laplace transform. The remaining integrand decreases rapidly as the imaginary parts of the three parameters increase in magnitude, so that a numerical evaluation of the integral seems feasible. An IBM-704 program is being prepared to carry out this computation.

I. ZEUS

General Program

With the development of the LASL Sherwood program, it became apparent that more and more energy would be required to supply the power for large-scale devices. In order to meet this expected demand, a program was established to design and construct a 12-megajoule capacitive energy storage system. This capacitor bank is designated by the name "Zeus." The construction program has been phased so that only one-half the bank is being installed at the present time with space being provided for the balance which will be installed later as the need arises. Power supplies and controls have been installed to handle the entire 12 megajoules.

Zeus is designed to provide discrete amounts of energy to four different experiments. Charging, discharging, timing, and firing controls have been provided together with suitable safety and monitoring systems. Considerable flexibility has been designed into the control system so that any program can utilize any one or more of four power supplies and 12 racks of capacitors. Only one experiment may be operated at a time but, once the initial cabling is installed, it will be a relatively simple operation to switch programs.

The bank, as presently installed, is divided into six megajoule racks with seven tiers on each. Each rack contains 336 capacitors with a total capacity of approximately 4900 μf. The maximum operating voltage is 20 kv, the peak design current is 3.36×10^6 amp per megajoule, ringing at 5 to 6 kc and decaying with 85% voltage reversal.

The following table gives the basic electrical characteristics for Zeus:

1 Tier	1 Rack
C = 700 μf	C = 4900 μf
V = 20 kv	V = 20 kv
W = 140,000 joules	W = 980,000 joules
L = 0.075 μh	L = 0.011 μh
R = 2×10^{-3} ohm	R = 0.28×10^{-3} ohm
48 capacitors	336 capacitors
16 ignitrons switches (Z-5385)	112 ignitrons switches

Design characteristics with external load

I_{peak} = 480,000 amp	$I_{peak} = 3.36 \times 10^{6}$ amp
K = 0.85 (i.e., 85% voltage reversal)	K = 0.85
R = 4×10^{-3} ohm	R = 5.72×10^{-4} ohm
L = 1.045 μh	L = 0.15 μh
T = 170 μsec	T = 170 μsec

Present Status

Installation of Zeus was started in August 1959 and to date ten of the 42 tiers have been completed and tested. Nine of these are being hooked up to the Perhapsatron S-5 and the circuits are being programmed and adjusted to operate this experiment. The balance of the installation is in various stages of completion and work is continuing. Only a limited amount of work will be possible, however, while the bank is in operation.

COMPONENT DEVELOPMENT

General Program

As research with the various Sherwood devices has progressed, there has been a constant demand for better components so that more

refined experiments can be performed. Included among these are capacitors and high-voltage, high-current switches. In the early stages of the program, there were no capacitors readily available commercially which would meet the requirements, and suitable capacitors had to be developed by industry. Gradually improvements in energy storage capacitors were made under the guidance of Sherwood engineers and physicists and now many varieties of improved capacitors are available. Still, there are experiments which require moderate numbers of low-inductance, high-Q, high-voltage capacitors which are not at present available. Therefore, a more intensive program has been established based on ideas and experiments at LASL which will bring in industry to work with LASL engineers and physicists towards understanding how to build better energy storage capacitors.

Similarly, the development of high-voltage, high-current switches for controlling the current from capacitor banks has progressed to fill the requirements of new research devices. The switch tube used in Zeus is an example. A successful research and development program for making a reliable 20-kv ignitron of relatively small size and high current carrying capacity was carried out in order to develop such a tube. The program is to be continued towards the development of a higher voltage unit. Along the same line, the multi-element spark gap has been developed to a high degree at LASL and further work is to be done, particularly on the small vacuum type gap.

Present Status

The development of better capacitors is taking a two-fold approach. Work has started on the development and test of a parallel plate type of unit with a simple geometry molded in plastic. Test samples show that this unit will provide a very low inductance with a much higher Q than has previously been obtained. Studies on where the losses occur in capacitors have led to ideas which are to be incorporated in the design and development of the following units:

Type I	Type II
C = 1 to 2 μf	C = 0.5 to 1 μf
V = 50 kv, ringing with 95% reversal	V = 100 kv, ringing with 95% reversal
f_r = 2 Mc	f_r = 5 Mc
Q = 30	Q = 200 at 5 Mc
Life - 5000 shots, guaranteed	Life - 5000 shots

In both types, the geometry must be optimized towards a low-inductance, coaxial configuration to which low-inductance transmission systems can be connected.